

Optimize sequencing depth for shotgun metagenomics of pollination system by rarefaction, using a modular profiling pipeline

Cong Liu

2021.8

A thesis submitted in partial fulfilment of the requirements for the degree of Master of Research at
Imperial College London

Submitted for the MRes in Computational Methods in Ecology and Evolution

Declaration:

All datasets used in this project are provided by Dr. Peter Graystock and the project was conducted under his supervision. I am responsible for the development and conduction of the analyses presented.

Abstract

Bee gut microbiome plays a crucial role in host health, involving in food digestion, pathogen defence and chemical detoxification. Vast relevant investigations use amplicon sequencing to explore bacterial diversity, while emergence of shotgun metagenomics offers unique advantages by capturing diversity of multiple taxonomic clades and providing information on function potentiality. However, utilization of shotgun metagenomics is hindered by complexity of data analysis and high cost of sequencing. Here, an integrated pipeline combining assembly-dependent and -independent methods was introduced for taxonomic and functional profiling of shotgun metagenomic data, and a framework of rarefaction and multimodel inference was constructed for optimizing sequencing depth. Both the pipeline and the framework were used for analysis of deep-sequencing datasets (2×150 bp read pairs) from honey bees, bumble bees and flower washes. The integrated pipeline illustrated taxon composition and metabolic potentiality of the metagenomes, and provided significant improvements in species identification. For species diversity estimation, about 40 and 43 million read pairs would be sufficient for metagenomic datasets from honey bees and bumble bees, respectively. If low leverage is given to rare species, shallower sequencing can be adopted. Function profiling is much less stable to sequencing depth than species content. Additional functional gene clusters (FGCs) were still being discovered at original sequencing depth of all samples. Overall, this project provides guidelines for defining a balance between sequencing cost and acquirement of reliable results for investigations of pollination system. Similar studies for other host species are recommended before undertaking metagenomic projects involving a large number of samples.

1 Introduction

Pollinators such as bees are crucial to maintain global food security and provide stability of natural systems (Hristov et al., 2020a, Bänisch et al., 2021, Khalifa et al., 2021) but their populations are facing declines (Brown and Paxton, 2009, Hristov et al., 2020b, Cheng and Ashton, 2021, Zattara and Aizen, 2021). A combination of stressors including parasites, pesticide exposure, invasive species, habitat loss and climate change is contributing to declines of bee populations. (Brown and Paxton, 2009, Hristov et al., 2020b, Cheng and Ashton, 2021, Zattara and Aizen, 2021).

Within the gut of bees, stable microbial communities (microbiomes) play crucial roles in food digestion, parasite defence and chemical detoxification (Moran, 2015, Engel et al., 2016, Raymann and Moran, 2018). They help mediate food digestion processes including polysaccharides breakdown (Zheng et al., 2019), sucrose hydrolysis (Engel et al., 2012, Lee et al., 2015), and mannose metabolism (Engel et al., 2012, Lee et al., 2015). Bee microbiomes also provide protection against pathogens including *Crithidia*, (Koch and Schmid-Hempel, 2011b, Cariveau et al., 2014), *Paenibacillus larvae*, (Ebeling et al., 2016, Forsgren et al., 2010) and *Nosema sp.* (Cariveau et al., 2014, Maes et al., 2016), and are involved in resistance to both

metal and metalloid toxins including cadmium (Rothman et al., 2019b), copper (Rothman et al., 2020) and selenate (Rothman et al., 2019a).

Amplicon sequencing, in which a species-specific barcode region is amplified and sequenced, is a powerful and vastly used method for investigations of microbiome compositions (Abdelfattah et al., 2018). In bee microbiome investigations, it is used to illustrate the taxonomic diversity of bee-associated bacteria and fungi (*e.g.* Geldert et al. (2021), Wang et al. (2021), Powell et al., Kapheim et al. (2021)). However, bees visit numerous niches during environment exploration and foraging activities, and can get contact with diverse eDNA signatures, which provide insight into pollinator ecology by reflecting interactions between bees and other organisms including bacteria, fungi, plants, arthropods and viruses (Bovo et al., 2018, Ribani et al., 2020, Bovo et al., 2020, Matsuzawa et al., 2020). It is difficult to explore this diversity via amplicon sequencing because it only captures a fraction of the whole community since analysis of different taxonomic groups is based on different barcode regions, *e.g.* 16S ribosomal RNA (rRNA) for bacteria (Hayashi et al., 2002, Eckburg et al., 2005), internal transcribed spacer (ITS) for fungi (Nilsson et al., 2008), cytochrome c oxidase subunit I (COI) for Animalia (Hebert et al., 2003) and plastid genes for plants (Group et al., 2009). As a result, amplicon sequencing only captures taxon diversity within a certain clade. Besides, it is difficult to illustrate function potentiality of bee-associated microbiome using amplicon sequencing since it does not provide information on content of functional gene clusters (FGCs), *i.e.* aggregates of genes with same function. As a result, functional capacity needs to be inferred based on taxon composition. Amplicon-based function predictors such as Tax4Fun (Aßhauer et al., 2015) and PI-CRUST (Douglas et al., 2018) predict functional capacity based on pre-sequenced genomes without taking gene content variation within taxa. However, bee bacterial symbionts are diversified at strain level (Engel et al., 2012, Powell et al., 2016, Ellegaard et al., 2020) and bacterial strains are often highly variable in gene content (Cordero and Polz, 2014, Brockhurst et al., 2019). As a result, amplicon-based inference of functional capacity of bee microbiome may not be reliable.

Shotgun metagenomics provides a solution for microbiome investigations to overcome drawbacks of amplicon sequencing. By capturing and sequencing DNA fragments unselectively, shotgun metagenomics is capable of providing comprehensive inventories of taxa and FGCs (Quince et al., 2017, New and Brito, 2020, Galloway-Peña and Hanson, 2020). However, utilization of shotgun metagenomics is hindered by challenges in bioinformatics. The goal of metagenomics is typically to provide a taxonomic and functional profile of the microbiome, and there is not a gold standard for performing metagenomic data analysis. Generally, one of the first steps in metagenomic analysis is assembling short reads into long contigs, which can help improve accuracy of metagenomic annotation (Wommack et al., 2008, Carr and Borenstein, 2014, Tran and Phan, 2020) and is necessary for discovery of novel taxa and genes (Culligan et al.,

2014, Youngblut et al., 2020). However, metagenome assembly is complex, compromised by fragmental assembly, chimaeras (Mikheenko et al., 2016) and loss of taxon/function diversity due to unassembled reads (Vollmers et al., 2017, Ayling et al., 2020). Probably because of these shortcomings, assembly is sometimes skipped and short reads are directly proceeded for annotation (Tringe et al., 2005, Abubucker et al., 2012, Vermote et al., 2018, Bovo et al., 2018), although the accuracy can be compromised due to low information load of short reads (Wommack et al., 2008, Carr and Borenstein, 2014, Tran and Phan, 2020). A combination of both assembly-dependent and -free methods could overcome the complexity and improving accuracy of metagenomic profiling (Becker et al., 2020).

A remaining challenge of metagenomics is the determination of a sequencing depth that provides reliable estimation of taxon/FGC diversity without overspending. It is recommended to retrieve as many reads as possible (Quince et al., 2017) since insufficient sequencing causes compromise in metagenome profiling (Cattonaro et al., 2018, Zaheer et al., 2018, Pereira-Marques et al., 2019, Gweon et al., 2019). However, deep metagenomic sequencing is expensive, which hinders its utilization, especially in large-scale projects. Currently, there are few published guidelines for the sufficient sequencing depth of a given environment or study type in order to reach a trade-off between sequencing effort and reliable output.

In order to balance sequencing cost and reliable estimation of taxon/FGC diversity, expected diversity represented by given sequencing depth need to be computed. Since a metagenomic dataset can be viewed as a random sample of an assemblage of genomic sequences, and profiling is the process by which reads are assigned to taxa or FGCs, the relationship between sequencing depth and diversity can be illustrated by rarefaction (randomly subsampling the original dataset without replacement) and quantified by model fitting, if the original dataset can provide an almost complete inventory of taxa/FGCs (Heck Jr et al., 1975, Hortal and Lobo, 2005, Gómez-Anaya et al., 2014, Hughes et al., 2021). The sequencing depth is sufficient for reliable estimation of taxon/FGC diversity if and only if the slope of the rarefaction curve is small (Hortal and Lobo, 2005, Chao and Jost, 2012, Roswell et al., 2021).

In this project, I utilised metagenomic datasets ($2 \times 150\text{bp}$) from three environmental types: the gut of honey bees (*Apis mellifera*), the gut of common North American bumble bees (*Bombus impatiens*) and the surface of a wild flower (*Erigeron annuus*). I aimed to (1) develop an integrated pipeline combining assembly-dependent and -independent methods to deliver improved taxon annotation of sequencing data and (2) optimize sequencing depth to balance sequencing cost and requirement for reliable analysis of microbial species diversity, or the description of their functional diversity. The integrated pipeline provided improvement in species identification compared with the assembly-dependent method. Rarefaction analysis showed that about 40/43 million clean read pairs would be a suitable compromise for sequencing honey/bumble bee samples and species diversity detection. Shallower sequencing can be adopted with

101 reduced emphasis on rare species. Functional profiling is more demanding about sequencing depth than
102 species profiling. Significant accumulation of FGCs was observed at final points of rarefaction curves from
103 all samples. These results provide guidelines for defining a balance between sequencing cost and obtain-
104 ing reliable taxonomic/functional profiles for metagenomic investigations of pollination system. Similar
105 studies for other host species are recommended before undertaking metagenomic projects with big sample
106 size.

107 **2 Materials and Methods**

108 **2.1 Samples, DNA extraction and sequencing**

109 Samples include four honey bees (two from the same hive (hive 13), one from a hive in the same apiary
110 (hive 15) and one caught foraging), three bumble bees from commercially supplied (Biobest) bumblebee
111 colonies (two from the same colony), and one buffer wash of a wild flower (*Erigeron annuus*).

112 DNA extraction was performed as in Graystock et al. (2020), followed by library preparation using a
113 low template protocol with Illumina Nextera Library Prep kits. Briefly, this involved tagmentation into
114 fragments of 300 bases before eight samples of 10ng were pooled together and sent to Beijing Genomics
115 Institute (BGI) for further quality control and sequencing using a full lane in the X-ten platform.

2.2 Metagenomic profiling using integrated pipeline

2.2.1 Integrated pipeline

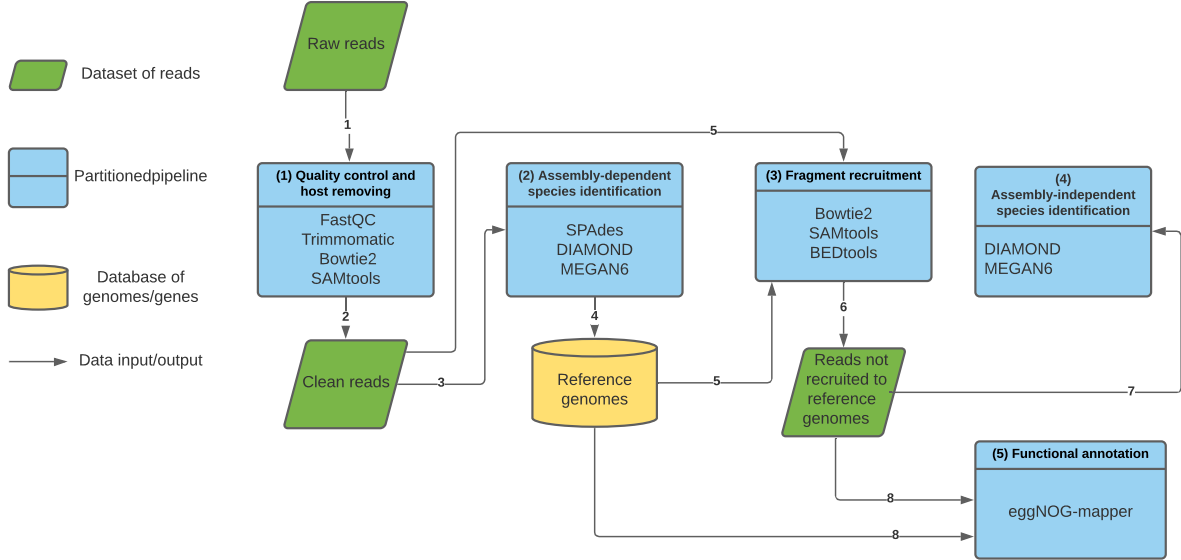


Figure 1: An overview of the integrated pipeline. The pipeline is separated into 5 modules, indicated by blue boxes. Green boxes indicate dataset of reads, while yellow boxes indicate database of genomes. Black arrows indicate the input and output of each step and the numbers on them indicate the order that each step is utilized.

I designed an integrated pipeline for shotgun metagenomic profiling, *i.e.* assigning reads to taxa or FGCs. It is separated into five modules (Figure 1).

In quality control and host removing, raw sequencing data quality is checked using FastQC v.0.11.5 (Andrews et al., 2010) and filtered by Trimmomatic v.0.39 (Bolger et al., 2014). Then clean reads are mapped to host genome using Bowtie2 v.2.4.2 (Langmead and Salzberg, 2012) and non-host reads are extracted by SAMtools v.1.11 (Li et al., 2009).

The non-host reads are subject to the module of assembly-dependent species identification. *De novo* assembly is conducted by SPAdes v.3.15.2 (Prjibelski et al., 2020). Assembled contigs are aligned to NCBI non-redundant (nr) database by DIAMOND v.2.0.7.145 (Buchfink et al., 2015), and assigned to taxa by MEGAN6 (Huson et al., 2007).

Then fragment recruitment is conducted to filter reads mapped to species represented by the assembly. A reference database is constructed and it comprises reference genome dataset, *i.e.* genomic sequences in FASTA format and corresponding genome annotation in general feature format (gff). For each species represented by assembly, its reference genome dataset, if available, is downloaded from NCBI using its

132 *datasets* command-line tool and added to the reference database. Then non-host reads are mapped to
 133 the reference database by Bowtie2, and unmapped reads are extracted by SAMtools.
 134 Reads not recruited by the reference database are subjected to assembly-independent species identification.
 135 They are aligned to NCBI nr database through DIAMOND and assigned to taxa by MEGAN6.
 136 Finally, functional annotation is conducted by EggNOG-mapper v.2.1.2 (Huerta-Cepas et al., 2017).
 137 It takes coding sequences (CDSs) of genomes in the reference database and reads subject to assembly-
 138 independent species identification as input and assigns them to Kyoto Encyclopedia of Genes and Genomes
 139 (KEGG) orthologies (KOs) (Kanehisa and Goto, 2000).
 140 The integrated pipeline was used for analysing metagenomic datasets involved in this study. Details in
 141 the pipeline and parameter settings of each module are described in Supplementary 7.1.

142 **2.2.2 Taxon/function quantification and metabolic pathway reconstruction**

143 After profiling, identified species and KOs were quantified by calculating relative sequence abundance, *i.e.*
 144 proportion of reads assigned to a species/KO in all reads annotated. For species without available reference
 145 genomes, their abundances were calculated using reads assigned to them in assembly-independent search.
 146 As for taxa with available reference genomes, they may be identified in both assembly-dependent and
 147 -independent search due to strain-specific genomic structures that are not present in reference genomes.
 148 Their abundances were calculated by summing number of reads that (1) mapped to coding sequences
 149 (CDSs) of reference genomes and (2) assigned to them in assembly-independent search. Reads mapped to
 150 non-coding regions were not taken into consideration in order to avoid overestimation since the assembly-
 151 independent search was based on aligning reads to nr database, which is composed of proteins. As for
 152 KO quantification, CDSs with zero coverage were excluded. Abundances of KOs were calculated by
 153 summing number of reads that (1) mapped to CDSs assigned to KOs and (2) assigned to KOs directly.
 154 Extraction of CDSs and calculation of their coverage were conducted by BEDtools v.2.30.0 (Quinlan and
 155 Hall, 2010).
 156 Metabolic pathways were inferred based on KOs. Reads assigned to plants and arthropods were not
 157 included since they were unlikely to represent living organisms. MinPath v.1.6 was used for pathway
 158 inference (Ye and Doak, 2009). It finds a minimal set of KEGG pathways that can explain all KOs
 159 provided as input.

2.3 Estimation of optimal sequencing depth required for metagenomic profiling

2.3.1 Simulating different sequencing depth by subsampling and diversity measured using Hill numbers

Species/KO inventories obtained from different sequencing depth was simulated by rarefaction. Since the ratio between numbers of raw and clean reads is dependent on sequencing process and is not influenced by sample type, sequencing depth here refers to number of clean read pairs to exclude variance caused by different proportion of low quality reads in samples of same type. Besides, the expected ratio between host and non-host reads in a metagenomic dataset is dependent on the DNA sample and not impacted significantly by sequencing depth. Thus the proportion of non-host reads in each simulation is expected to be the same with that in the original dataset.

Based on these considerations, I randomly subsampled non-host dataset of each sample, taking 10%-100% of read pairs at interval of 10% by *reformat.sh* script of BBmap v.38.90 (Bushnell, 2014), and profiled subsampled datasets by the integrated pipeline (Figure 1). The sequencing depth of each subsampled dataset equals number of subsampled non-host read pairs divided by ratio between non-host and clean read pairs. Thus, each subsampled dataset of non-host reads is corresponded to an imaginary dataset of clean reads, whose proportion of non-host reads is the same with that of the original metagenomic dataset.

After profiling subsampled datasets, species/KO diversity was measured by Hill number, a parametric family of diversity indexes differing by order q (Hill, 1973, Ma and Li, 2018, Roswell et al., 2021). Hill numbers provide unique advantages over other diversity indexes (Chao et al., 2014a,b, Alberdi and Gilbert, 2019, Roswell et al., 2021). First, Hill numbers follow a replication principle: if a proportion of categories in an inventory was removed randomly, all Hill numbers are expected to decrease by that proportion. Second, the sensitivity of Hill numbers to relative abundances can be modulated by order q . Third, widely used diversity indexes including species richness, Shannon index and Simpson index, can be converted to Hill numbers through algebraic transformations.

Hill number of order q is defined as Equation 1 (Hill, 1973).

$$D^{(q)} = \left(\sum_i (p_i)^q \right)^{\frac{1}{1-q}} \quad (1)$$

p_i represents the relative abundance of i th species/KO. When $q = 0$, abundances are not taken into consideration and $D^{(0)}$ equals species/KO richness. When $q = 1$, emphasis is given to species/KOs with general abundances. Hill number is defined as the limit of Equation 1 as q tends to 1 and equals the

189 exponential of Shannon index (2).

$$D^{(1)} = e^{-\sum_i p_i \log p_i} \quad (2)$$

190 When $q = 2$, high leverage is provided to abundant species/KOs and Hill number equals the inverse of
191 Simpson index (Equation 3).

$$D^{(2)} = \frac{1}{\sum_i (p_i)^2} \quad (3)$$

192 **2.3.2 Quantification of relationship between sequencing depth and Hill numbers by fitting** 193 **rarefaction curves**

194 Hill number of order q (Equation 1) measures diversity of an inventory as the number of equally abundant
195 categories in an imaginary inventory with the same diversity (Chao et al., 2014a, Roswell et al., 2021).
196 Order q determines leverage given to abundant categories. All Hill numbers behave in the following way:
197 removing a proportion of categories in an inventory randomly is expected to cause decrease of Hill numbers
198 in that proportion (Roswell et al., 2021). Thus, it can be hypothesized that as sequencing depth (number
199 of clean read pairs) increases, the detection of novel species/KOs leads to increase of Hill numbers, and
200 when sequencing depth is so big that all species/KOs present in the metagenomic DNA sample have been
201 detected, Hill numbers level off. Such a relationship can be fitted by asymptotic species accumulation
202 models.

203 Let Hill number of order q (Equation 1) be a function of sequencing depth x , which takes million read pairs
204 as the unit. This function was fitted using a multimodel inference method. First, a total of five candidate
205 models (Table S1) were fitted to rarefaction curves which plots Hill numbers against sequencing depth. R
206 package *minpack.lm* v.1.2.1, which employs Levenberg-Marquardt nonlinear least-square algorithm, was
207 used for model fitting. Then small sample unbiased Akaike information criterion (AICc) (Anderson, 2007)
208 of each candidate model was calculated (Equation 4):

$$AICc = -2L + 2k + \frac{2k(k+1)}{(n-k-1)} \quad (4)$$

209 where n is number of observed data points ($n = 10$ in this study), k is the number of fitted coefficients,
210 and L is maximized log-likelihood, given by Equation 5.

$$L = -0.5n \log\left(\frac{Rss}{n}\right) \quad (5)$$

211 Rss represents residual sum of squares.

212 Then model averaging was conducted. First, differences of AICc scores between i th candidate models and

the model with lowest AICc value were calculated using Equation 6.

$$\Delta_i = AICc_i - AICc_{min} \quad (6)$$

$AICc_i$ is the AICc score of i th plausible model and $AICc_{min}$ is the lowest AICc score among all candidate models. The Akaike weight of i th model is given by Equation 7 (Anderson, 2007).

$$w_i = \frac{e^{(-0.5\Delta_i)}}{\sum_i e^{(-0.5\Delta_i)}} \quad (7)$$

Denote i th candidate model by $D_i^{(q)} = D_i^{(q)}(x)$, the averaged model is given by Equation 8.

$$D^{(q)}(x) = \sum_i w_i D_i^{(q)}(x) \quad (8)$$

The slope of rarefaction curve was calculated by first derivative of averaged model (Equation 9). It reflects the increase rate of the curve.

$$\frac{dD^q}{dx} = \sum_i w_i \frac{dD_i^{(q)}}{dx} \quad (9)$$

The asymptote of rarefaction curve as sequencing depth tends to infinity is given by Equation 10. It provides an estimation of the total diversity and is comparable among metagenomic DNA samples with different sequencing depth. However, the accuracy of asymptotic estimators is controversial (Colwell and Coddington, 1994, Chazdon et al., 1998, Jimenez-Valverde et al., 2006, Hortal et al., 2006).

$$\lim_{x \rightarrow +\infty} D^{(q)}(x) = \sum_i w_i \lim_{x \rightarrow +\infty} D_i^{(q)}(x) \quad (10)$$

2.3.3 Estimating optimal sequencing depth using rarefaction curves

Optimal sequencing depth is defined as the point at which diversity starts to level off as sequencing depth increases, and its precise estimation via rarefaction is based on the assumption that the original dataset is sufficient for detection of almost all species/KOs present. This assumption can be verified by looking at the rarefaction curve that plots species/KO richness (Hill number of order 0) against sequencing depth. The original dataset is sufficient for providing a reliable inventory if and only if the rarefaction curve of richness is characterized by a small final slope (Heck Jr et al., 1975, Hortal and Lobo, 2005, Chao and Jost, 2012). Then an estimation of optimal sequencing depth is provided by the point at which the slope of rarefaction curve decreases to a given cut-off value (Hortal and Lobo, 2005, Gómez-Anaya et al., 2014).

232 3 Results

233 3.1 Sequence reads

234 Eight samples (four honey bees, three bumble bees and one flower eDNA) were sequenced. The quality
235 reports of raw reads showed low-quality 3'-end (Figure S1a), uneven base content in 5'-end (Figure S1b)
236 and the present of adaptors (Figure S1c). The quality control procedure covered these aspects and
237 improved data quality (Figure S1d, S1e and S1f).

238 After quality control, read pairs aligned to host genome were removed. Table S2 reports numbers of
239 raw, clean and non-host read pairs. Honey bee sample *Bee-Amellifera_13_1* was filtered from further
240 analysis since its low raw read pair number (1.10 million compared to the other samples at 59 million) is
241 suggestive of a poor quality sample. After quality control, 62.08%-76.52% of raw read pairs were retained
242 for these three honey bee samples. Then a different proportion of non-host read pairs (29.52%-86.19%)
243 were retained from each sample. As for bumble bee samples, about 58 million raw read pairs were obtained
244 for each sample and 82.1%-83.8% were retained after quality control. After host removing, 7.35%-10.08%
245 of clean reads were retained. For flower eDNA sample, 1.44 million raw read pairs were obtained and
246 61.15% of them were retained. Host removing was not conducted because it is a sample of eDNA washed
247 from flower surface.

248 3.2 Application of integrated pipeline

249 The integrated pipeline was used to profile metagenomic datasets from pollination system, illustrating its
250 capacity in presenting taxon composition and functional potentiality of microbiome. Although samples
251 are different in proportion of host contamination (Table S2, Figure 2a), diverse communities composed of
252 multiple taxonomic clades were identified (Figure 2b). Most species identified are common in pollination
253 system. Their present indicate that samples were of good quality and representative for microbiomes from
254 pollination system.

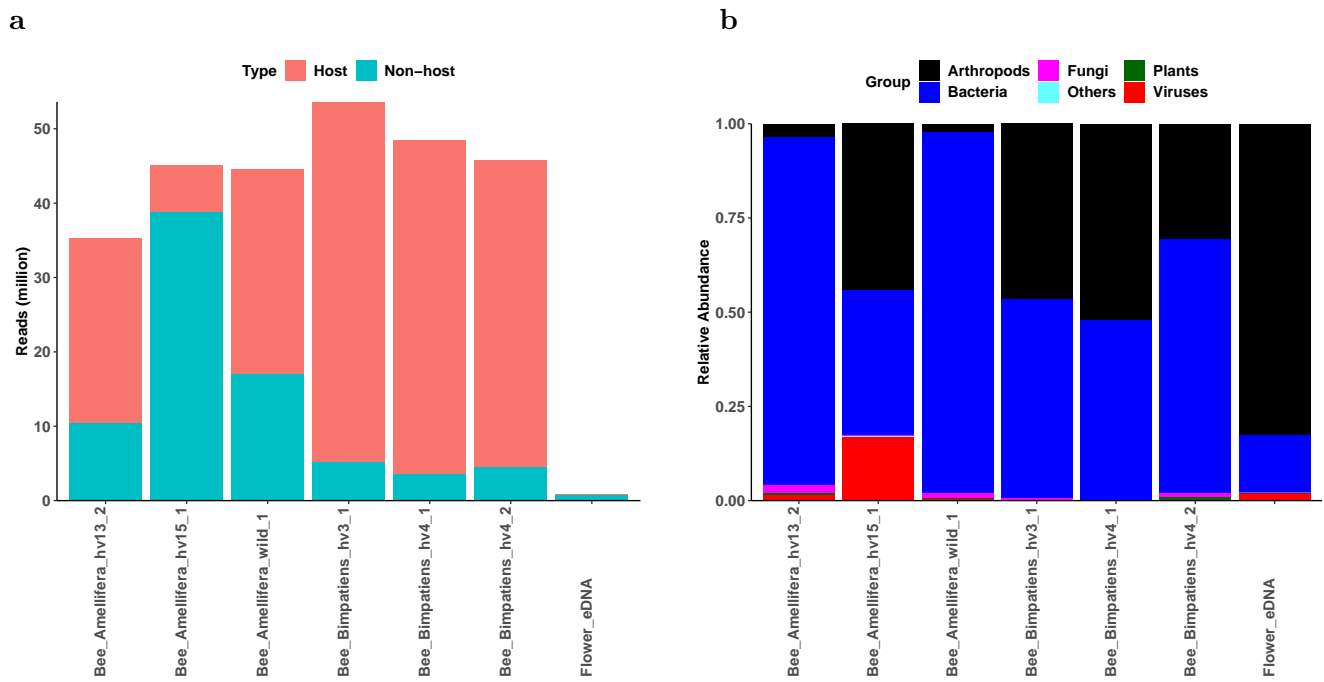


Figure 2: The number of host and non-host reads in each sample (a) and the relative abundance of species under six taxonomic groups (b): superkingdom Viruses, superkingdom Bacteria, kingdom Viridiplantae (plants), kingdom Fungi, phylum Arthropoda and others (species that are not in the other five groups).

255 The presence of known core members of bee-associated bacterial community including species within
 256 *Bifidobacterium*, *Frischella*, *Gilliamella*, *Snodgrassella*, *Lactobacillus*, *Apilactobacillus* and *Bombilacto-*
 257 *bacillus* (Figure 3) (Koch and Schmid-Hempel, 2011a, Moran, 2015, Kwong et al., 2017, Zheng et al.,
 258 2020) suggests good sample quality. As for other abundant bacteria, *Fructobacillus sp.* are often found
 259 in fructose-rich environments like flowers (Endo and Dicks, 2014); *Bartonella apis* is related to animal
 260 pathogens (Kešnerová et al., 2016) and is widespread in honey bee workers (Raymann and Moran, 2018);
 261 *Candidatus Schmidhempelia bombi* is a known uncultured symbiont of *Bombus impatiens* (Martinson
 262 et al., 2014). It should be noted that some typical bee-associated bacteria were also found on the flower,
 263 including *Bartonella apis*, *Bifidobacterium asteroides*, *Bombilactobacillus mellis* and *Gilliamella apicola*.
 264 Composition of arthropods and plants indicating interactions within pollination networks. Most arthro-
 265 pods identified are pollinators within *Apis* and *Bombus* (Figure S2). However, some of them might be
 266 considered as false positive. For example, *Apis cerana*, *Apis dorsata* and *Apis florea* are mainly found in
 267 Asia and unlikely to present in the area where samples were collected. These might derive by similarity
 268 between genomes of *Apis mellifera* and other *Apis* species. As for plant species (Figure S3), they indicate
 269 foraging areas of bees. Several crop species were identified, including *Brassica napus* (rape), *Brassica*
 270 *oleracea*, *Cicer arietinum* (chickpea), *Glycine max* (soybean), *Helianthus annuus* (sunflower), *Nicotiana*
 271 *sylvestris* (flowering tobacco) and *Raphanus sativus* (radish).

272 Fungal and virus species were identified. In fungal communities of most samples, *Nosema ceranae*, a
 273 widespread bee pathogen, was the dominant species. (Figure S4). Besides, three yeast species (*Clavispora*
 274 *lusitaniae*, *Saprochaete ingens* and *Wickerhamiella sorbophila*) were also found in bees. As for viruses,
 275 most of them are phages or arthropod-infecting species (Figure S5). Phage species include *Bifidobac-*
 276 *terium phage BitterVaud1* infecting bee-commensal bacterium *Bifidobacterium asteroides* (Bonilla-Rosso
 277 et al., 2020); *Bacteriophage sp.* infecting *Pseudomonas aeruginosa* (Essoh et al., 2015), an opportunistic
 278 pathogen that might contaminate bees (Bailey, 1968, Papadopoulou-Karabela et al., 1992, 1993); and un-
 279 classified species within Myoviridae and Siphoviridae. Listed arthropod-infecting viruses including *Apis*
 280 *mellifera filamentous virus* and *Bombus cryptarum densovirus* that infect bees; and several parvoviruses
 281 (*Blattodean pefuambidensovirus 1*, *Hemipteran scindoambidensovirus 1*, *Hymenopteran scindoambidenso-*
 282 *virus 1* and *Orthopteran scindoambidensovirus 1*) (Pénzes et al., 2020).

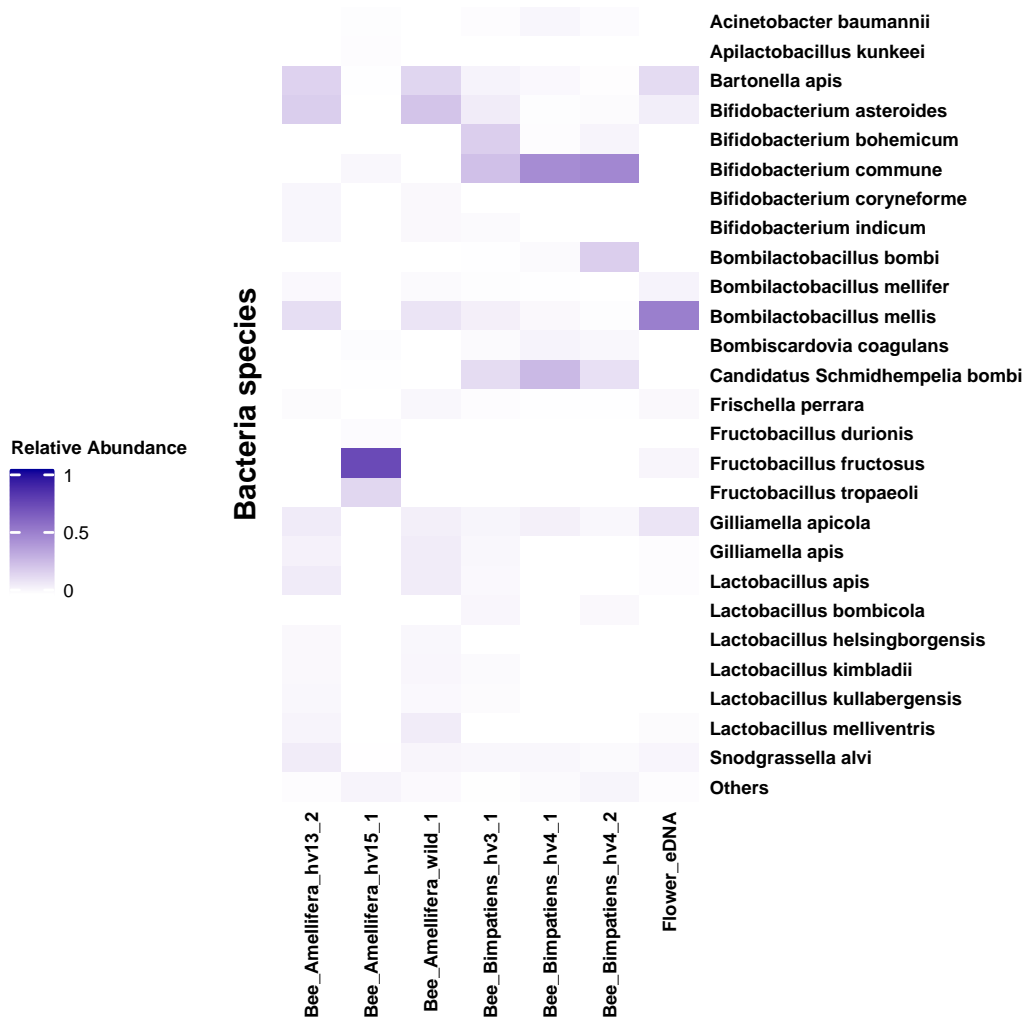


Figure 3: Heatmaps for bacterial species abundance distribution in all samples. The relative abundance takes reads assigned to bacterial species as background. Species with relative abundance smaller than 1% in all samples are collapsed as "others".

283 The integrated pipeline also provides information on FGC content, which shows function potentiality
 284 of metagenome. Here FGC content was represented by identified KOs, which were used for KEGG
 285 pathway inference in order to illustrate metabolic potentiality of metagenomic samples. Reads assigned to
 286 plants and arthropods were not involved in pathway inference since they are unlikely to represent living
 287 organisms. The coverage of a pathway was calculated by the ratio between number of annotated KOs
 288 and total number of KOs involved in that pathway.

289 Here concern is given to metabolism pathways of carbonhydrates and amino acids, which are crucial for
 290 bee health. Inferred pathways indicate potential capability of metabolism of sugars including fructose,
 291 sucrose, mannose and galactose (Figure S6), and all ten essential amino acids for honey bees (*i.e.* arginine,
 292 histidine, isoleucine, leucine, lysine, methionine, phenylalanine, threonine, tryptophan and valine) (Figure
 293 S7) (Groot, 1953).

294 3.3 Evaluation of performance of integrated pipeline in species identification

295 The performance of integrated pipeline in species identification was evaluated by comparing it with
 296 assembly-dependent method, using rarefied datasets. In integrated pipeline (Figure 1), clean non-host
 297 reads are first assembled to into contigs and assigned to taxa. Then a reference database composed of
 298 genomes of assembly-represented species is constructed. Reads not aligned to the reference database
 299 are subjected to assembly-independent taxon search. The reference database and assembly-independent
 300 search helped improve species identification in all three sample types, especially in simulations of low
 301 sequencing depth (Figure 4).

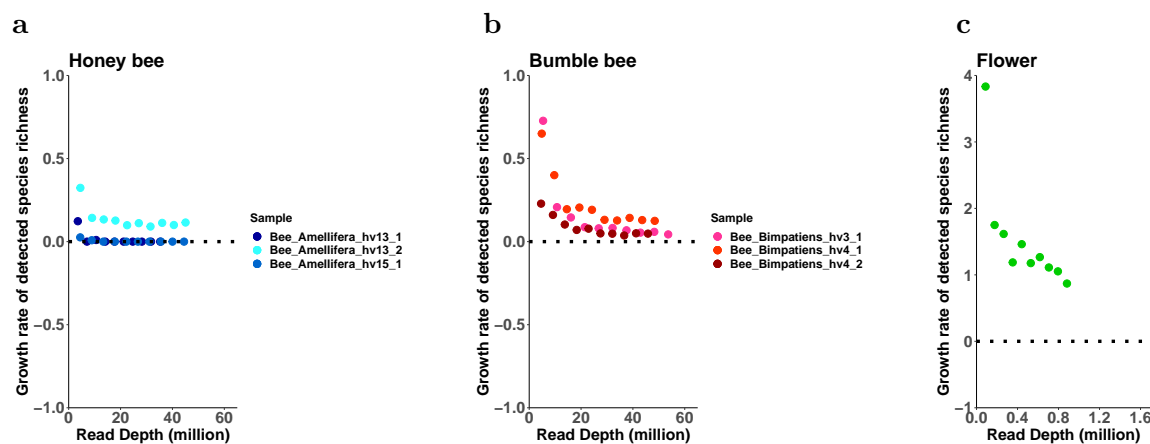


Figure 4: Integrated pipeline improves the detection of species richness. The horizontal axis represents sequencing depth, and the vertical axis represents growth rate of detected species richness comparing the integrated pipeline and assembly-dependent species identification. Different sequencing depth was simulated by rarefaction. Sample type is shown in the top left of each subfigure.

3.4 Optimal sequencing depth required for detection of species and function diversity

In order to determine the influence of sequencing depth and thus optimize sequencing depth for analysing taxonomic and functional diversity, rarefaction analysis was conducted. Different sequencing depth was simulated by randomly subsampling original datasets at proportions from 10% to 90% at an interval of 10%. The relationship between sequencing depth (clean read pair number) and species/KO diversity (Hill numbers of order 0, 1, 2) was quantified by fitting and averaging asymptotic species accumulation models. The slope of the model reflects the increase rate of diversity. The point at which it drops to a cut-off value provides an estimation of optimal sequencing depth. Besides, the asymptote of the model as sequencing depth tends to infinity provides an estimation of total diversity.

Rarefaction assumes that the original dataset provides an almost complete inventory, which can be verified by final slope of rarefaction curve for Hill number of order 0 (richness). Figure 5 shows rarefaction curves for species/KO richness and Table 1 summarizes their final slopes. For species diversity rarefaction, all bumble bee samples are sufficient, with final slopes < 0.1 and completeness (ratio between final richness and asymptote) > 0.98 . As for honey bees, *Bee_Amellifera_hv15_1* and *Bee_Amellifera_wild_1* are sufficient, while *Bee_Amellifera_hv13_2* is insufficient, with final slope > 1 and completeness < 0.8 . For the flower eDNA sample, the final slope of species richness rarefaction curve is 10.8380 and its completeness is 1.32%, indicating more sequencing effort is needed for species profiling. As for function diversity rarefaction, the final slopes of all KO richness rarefaction curves are higher than 15, indicating no dataset can providing an almost complete inventory of KOs. Thus, estimation of optimal sequencing depth was conducted for the combinations of two sample types (honey bee and bumble bee) and one study type (species profiling), based on five datasets (two honey bees and three bumble bees).

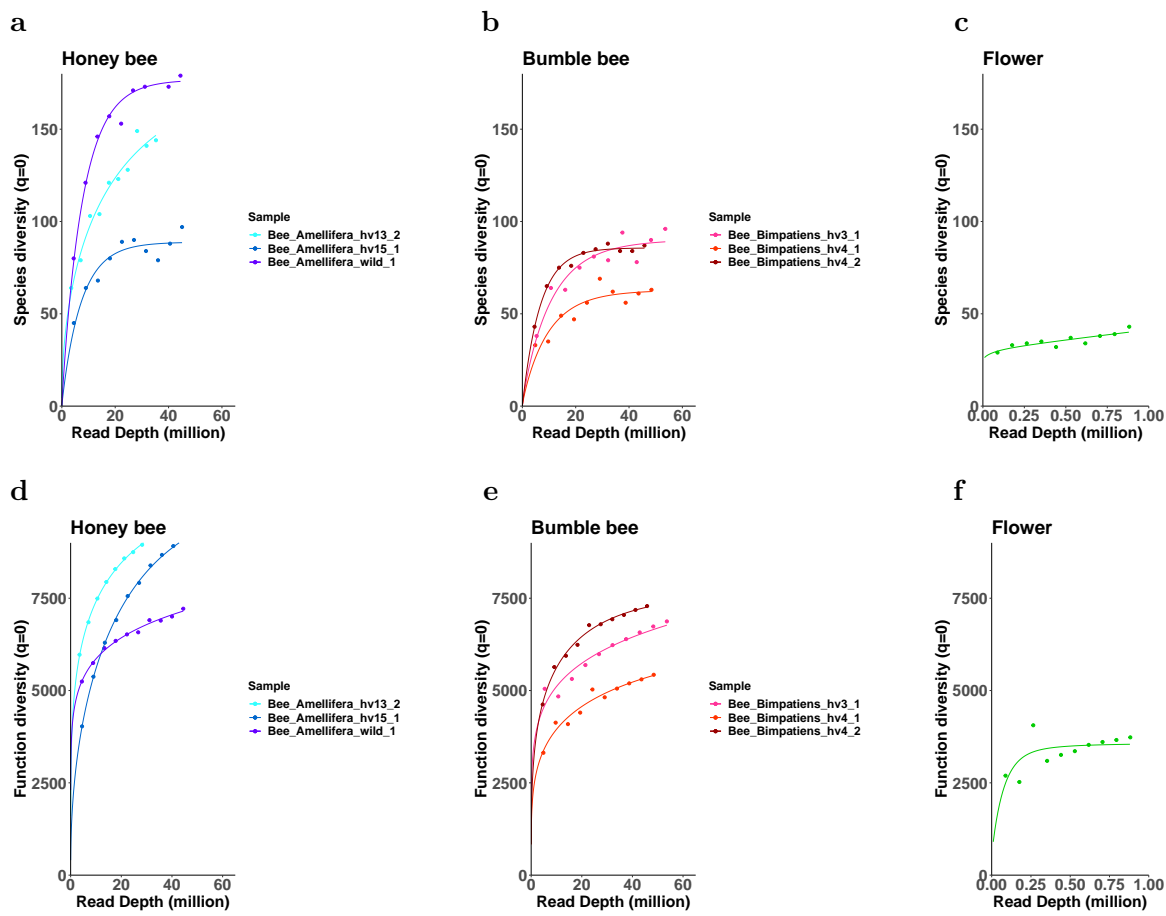


Figure 5: Rarefaction curves for species (a, b, c) or Kyoto Encyclopedia of Genes and Genomes (KEGG) orthologies (KOs) (d, e, f) richness (Hill number of order 0). The horizontal axis represents sequencing depth, and the vertical axis represents richness. Sample type is shown in the top left of each subfigure. Note that the scale of horizontal axis in subfigure c and f is much smaller than that in other subfigures.

Table 1: Summary of final point of rarefaction curve for richness (Hill number of order 0) of species or Kyoto Encyclopedia of Genes and Genomes (KEGG) orthologies (KOs). Type: indicates whether this row reports rarefaction curve for species or KO richness. Depth: sequencing depth taking million read pairs as unit. Observed richness: observed species/KO richness. Expected richness: expected species/KO richness predicted by modelling rarefaction curve. Final slope: final slope of rarefaction curve. Asymptote: asymptote as sequencing depth tends to infinity, calculated by modelling rarefaction curve. Completeness: ratio between expected richness and asymptote.

Sample	Type	Depth	Observed richness	Expected richness	Final slope	Asymptote	Completeness
<i>Bee_Amellifera_hv13_2</i>	species	35.28	144	146.69	1.0958	184.94	0.7931
<i>Bee_Amellifera_hv15_1</i>	species	45.05	97	88.53	0.0344	88.84	0.9966
<i>Bee_Amellifera_wild_1</i>	species	44.46	179	175.89	0.0991	176.84	0.9946
<i>Bee_Bimpatiensi_hv3_1</i>	species	53.61	96	89.00	0.0897	90.79	0.9803
<i>Bee_Bimpatiensi_hv4_1</i>	species	48.42	63	62.06	0.0626	62.92	0.9862
<i>Bee_Bimpatiensi_hv4_2</i>	species	45.80	87	85.59	0.0146	85.69	0.9988
<i>Flower_eDNA</i>	species	0.88	43	40.04	10.8380	3034.88	0.0132
<i>Bee_Amellifera_hv13_2</i>	KO	35.28	9289	9284.45	38.6844	10641.27	0.8725
<i>Bee_Amellifera_hv15_1</i>	KO	45.05	9046	9102.78	43.8717	10453.98	0.8707
<i>Bee_Amellifera_wild_1</i>	KO	44.46	7216	7151.72	21.4368	14779.89	0.4839
<i>Bee_Bimpatiensi_hv3_1</i>	KO	53.61	6872	6769.80	21.1588	28111.79	0.2408
<i>Bee_Bimpatiensi_hv4_1</i>	KO	48.42	5427	5410.71	19.6932	7665.58	0.7058
<i>Bee_Bimpatiensi_hv4_2</i>	KO	45.8	7288	7259.56	15.6309	7873.64	0.9220
<i>Flower_eDNA</i>	KO	0.88	3732	3544.54	60.4367	3571.11	0.9926

Optimal sequencing depth is estimated by the point at which the slope of rarefaction curve drops to a cut-off value. Table 2 summarizes estimations of optimal sequencing depth for detection of species diversity, using 0.5, 0.1, 0.05 and 0.01 as cut-off values. When order q of Hill number equals 0, *i.e.* species abundances are not considered, cut-off value of 0.1 for slope of rarefaction curve is sufficient for providing completeness $> 97\%$ in all samples. The average optimal sequencing depth are 40.33 million for honey bees and 42.49 million for bumble bees. When species abundances are considered (order q equals 1 or 2), cut-off value of 0.01 can provide completeness $> 95\%$ in most pairs of sample and q value. For honey bees, the average optimal sequencing depth are 18.57 million ($q = 1$) and 17.45 million ($q = 2$). For bumble bee samples, the average optimal sequencing depth are 40.33 million ($q = 1$) and 24.77 million ($q = 2$).

Table 2: Summary of optimal sequencing depth estimated from different cut-off values of slope. Optimal sequencing depth was estimated by the point at which the slope of rarefaction curve drops to a cut-off value (0.5, 0.1, 0.05 or 0.01). q : order of Hill number that determines sensitivity to species abundances. Asymptote: asymptote as sequencing depth tends to infinity, calculated by modelling rarefaction curve. Depth: optimal sequencing depth taking million read pairs as unit. Expected diversity: expected Hill number provided by the optimal sequencing depth. Completeness: ratio between expected diversity and asymptote.

Sample	q	Asymptote	Slope < 0.5			Slope < 0.1			Slope < 0.05			Slope < 0.01		
			Depth	Expected diversity	Completeness	Depth	Expected diversity	Completeness	Depth	Expected diversity	Completeness	Depth	Expected diversity	Completeness
<i>Bee_Amellifera_hv15_1</i>	0	88.84	23.54	84.85	0.9551	36.27	87.99	0.9905	41.95	88.40	0.9951	55.75	88.74	0.9989
<i>Bee_Amellifera_wild_1</i>	0	176.84	30.53	172.46	0.9752	44.39	175.88	0.9946	50.57	176.33	0.9971	65.86	176.70	0.9992
<i>Bee_Amellifera_hv15_1</i>	1	12.28	3.18	10.67	0.8699	5.83	11.33	0.9224	7.21	11.43	0.9304	15.21	11.58	0.9429
<i>Bee_Amellifera_wild_1</i>	1	14.77	0.69	13.49	0.9137	3.30	14.03	0.9498	6.20	14.23	0.9635	21.93	14.58	0.9868
<i>Bee_Amellifera_hv13_1</i>	2	4.85	0.02	4.26	0.8789	0.20	4.29	0.8848	0.94	4.34	0.8950	4.27	4.42	0.9115
<i>Bee_Amellifera_hv13_2</i>	2	11.00	4.47	10.15	0.9232	7.20	10.83	0.9845	8.38	10.91	0.9922	11.14	10.98	0.9984
<i>Bee_Bimpatiensi_hv3_1</i>	0	90.79	30.80	83.69	0.9218	52.03	88.85	0.9786	62.56	89.61	0.9870	92.35	90.32	0.9948
<i>Bee_Bimpatiensi_hv4_1</i>	0	62.92	24.83	57.22	0.9093	42.76	61.61	0.9791	51.24	62.22	0.9887	73.55	62.76	0.9973
<i>Bee_Bimpatiensi_hv4_2</i>	0	85.69	21.75	82.30	0.9604	32.67	85.01	0.9920	37.39	85.35	0.9960	48.40	85.62	0.9992
<i>Bee_Bimpatiensi_hv3_1</i>	1	21.59	3.63	10.50	0.4862	9.47	11.76	0.5449	15.37	12.18	0.5639	58.09	13.04	0.6040
<i>Bee_Bimpatiensi_hv4_1</i>	1	11.85	3.80	9.45	0.7973	10.15	10.87	0.9174	14.68	11.19	0.9445	31.22	11.57	0.9766
<i>Bee_Bimpatiensi_hv4_2</i>	1	12.66	4.17	10.24	0.8087	10.47	11.67	0.9213	14.85	11.98	0.9458	31.68	12.36	0.9760
<i>Bee_Bimpatiensi_hv3_1</i>	2	8.73	2.20	6.16	0.7051	6.28	7.06	0.8088	9.45	7.28	0.8344	23.89	7.60	0.8708
<i>Bee_Bimpatiensi_hv4_1</i>	2	8.33	3.12	6.28	0.7540	8.52	7.50	0.9002	12.30	7.76	0.9323	26.68	8.09	0.9718
<i>Bee_Bimpatiensi_hv4_2</i>	2	7.12	2.90	5.34	0.7493	7.47	6.38	0.8961	10.58	6.60	0.9270	23.73	6.90	0.9683

4 Discussion

Here, I constructed an integrated pipeline combining assembly-dependent and -independent methods for taxonomic and functional profiling of shotgun metagenomics, and applied it to analysis of metagenomes from honey bees, bumble bees and flower washes. The profiling results showed that the integrated pipeline is able to determine a comprehensive view of the taxonomic diversity (across multiple clades) and infer functional potentiality of metagenome by providing information on FGC content. The developed method is more sensitive to species identification compared with standard assembly-dependent methods. Then I computed expected species/FGC diversity represented by given sequencing depth through rarefaction analysis, in order to optimize sequencing depth to balance cost and reliability of analysis results. Optimal sequencing depth differs by types of samples and investigations. For estimation of species diversity, sequencing depth can be optimized especially when low leverage is given to rare species. As for functional profiling, deeper sequencing depth is required.

The integrated pipeline for taxonomic and functional profiling of metagenome provides several advantages. First, through combination with assembly-free taxon search, it helps solve high false negative rate associated with assembly-dependent species identification, which is caused by reads left unassembled. This was shown by analysing real metagenomic datasets from pollination system and simulating differ-

ent sequencing depth by rarefaction. Second, the modularity of integrated pipeline provides flexibility for incorporation of alternative tools. For example, BWA aligner (Li and Durbin, 2009) serves as an alternative for Bowtie2, and SPAdes can be replaced by other metagenomic assemblers such as Megahit (Li et al., 2015) and IDBA-UD (Peng et al., 2012). Third, the output files generated by each step are recorded and can be inspected easily, which provides transparency for troubleshooting. However, the performance of integrated pipeline would to be evaluated more comprehensively by further analysis of different datasets and comparison with other profiling strategies. Metagenomes from other host species could be used to illustrate the performance of integrated pipeline. Standardized mock metagenomes, even though they are less complex than real ones, could also be used to benchmark sensitivity and accuracy of integrated pipeline since it is an artificial metagenome with predefined diversity, generated by combining known sequences from different species (Vollmers et al., 2017, Sczyrba et al., 2017, Becker et al., 2020). Further, the performance of integrated pipeline in metagenome profiling could be further benchmarked against other analysis strategies, such as MG-RAST (Meyer et al., 2008), SqueezeMeta (Tamames and Puente-Sánchez, 2019) and Kraken (Wood and Salzberg, 2014).

The integrated pipeline was used to analyse metagenomes of bees and flower washes, illustrating their taxon composition and metabolic potentiality. Bee-associated microorganisms were identified in flower washes, including both pathogens (*e.g. Nosema ceranae* and *Apis mellifera filamentous virus*) and symbionts (*e.g. Bifidobacterium asteroides*, *Bombilactobacillus mellis* and *Gilliamella apicola*). Flowers have been indicated as hubs for transmission of bee pathogens (Durrer and Schmid-Hempel, 1994, Koch et al., 2017, Graystock et al., 2020). Through shared flower use, multiple pathogens transmit between pollinators, including *Nosema ceranae* (Graystock et al., 2015) and *Crithidia bombi* (Figuerola et al., 2019). There is also growing evidence for present of bee symbionts on flower (McFREDERICK et al., 2012, McFrederick et al., 2017, Keller et al., 2020, Vannette, 2020). However, its role in bee microbiome assembly and functional importance in pollination remains an open question (Keller et al., 2020, Vannette, 2020). As for function profiling, it is indicated that bee-associated microbiome is capable of metabolizing carbohydrates such as glucose, fructose, sucrose and mannose. Carbohydrates are main component of bee diet and microbiome-mediated carbohydrate-processing have been vastly investigated (Engel et al., 2012, Lee et al., 2015, 2018, Taylor et al., 2019). Besides, pathways for metabolism of all ten essential amino acids for honey bees (Groot, 1953) were inferred. Essential amino acids are crucial for bee health (Simcock et al., 2014, Paoli et al., 2014, Stabler et al., 2015, Hendriksma et al., 2019) and influence feeding preference due to their potential deficiency in single pollen source (Cook et al., 2003, Hendriksma et al., 2014, Hendriksma and Shafir, 2016). Whether bee-associated microbiome influences host health by providing amino acids need to be further investigated.

Optimization of sequencing depth is important for shotgun metagenomics since insufficient sequencing causes underestimation of taxonomic/functional diversity (Cattonaro et al., 2018, Zaheer et al., 2018, Gweon et al., 2019, Pereira-Marques et al., 2019), while deep sequencing is of high cost. Here, expected species/KO diversity provided by given sequencing depth was estimated by rarefaction and model fitting, using datasets from honey bees, bumble bees and flower washes. It was shown that increasing sequencing depth boosted identification of species/KO, highlighting value of deep metagenomic sequencing. For function profiling, no dataset involved here is big enough to provide an almost complete inventory of KOs even though most samples were deeply sequenced, indicating such task is demanding about sequencing depth. Therefore, when dealing with function potentiality of microbiome associated with bees or flowers, retrieving as many reads as possible would be recommended. As for species profiling, although deep sequencing is still valuable, sequencing depth can be optimized when the budget is limited, especially when low leverage is given to rare species. For honey bees, approximate 40 million sequencing depth (12 Gbp) can be sufficient for representing species richness. When assessing biodiversity with reduced emphasis on rare species, 17-19 million sequencing depth (5.1-5.7 Gbp) can provide robust estimation. As for bumble bees, about 40-43 million sequencing depth (12-12.9 Gbp) can provide reliable estimation for species richness and diversity index with emphasis on species of general abundance, and about 25 (7.5 Gbp) million sequencing depth can be sufficient for estimation of biodiversity with high leverage on abundant species. It should be noted that the efficacy of optimal sequencing depth estimation is reduced by limited number of samples. Here, honey bee and bumble bee associated microbiome was represented by only three samples, and there was only one sample of flower eDNA. However, microbiomes of pollination system are highly dynamic and variable in diversity. To generate reliable guideline for sequencing depth optimization, more samples need to be evolved. Besides, there is a lack of repeat in sequencing depth subsampling. Repeated subsampling boosts precise computation of rarefaction curve and increases accuracy of estimation of optimal sequencing depth.

5 Conclusion

Shotgun metagenomics is capable of illustrating diversity of multiple taxonomic clades and gene content, and thus provides unique advantages over vastly used amplicon sequencing, particularly for investigations of highly diverse microbial communities. However, utilization of shotgun metagenomics is hindered by challenges in data analysis and high cost of sequencing. Here, I constructed an integrated pipeline for analysis of shotgun metagenomic data. It provides benefits in terms of results, flexibility and transparency. I also constructed a framework for optimizing depth of shotgun metagenomic sequencing in order to balance high cost of sequencing and reliability of analysis results. The pipeline and the framework were

413 used for analysis of real datasets from pollination system. For species diversity detection, about 40 million
414 clean 2×150 bp read pairs would be sufficient honey bee samples to balance sequencing cost and reliable
415 output; and 43 million would be sufficient for sequencing bumble bee samples. Shallower sequencing can
416 be adopted with reduced emphasis on rare species. As for functional profiling, obtaining as many reads as
417 possible would be the recommendation. These results provide guidelines for cost-effective metagenomic
418 investigations of bee microbiomes. Methods used in this project can be adopted to similar studies for
419 other host species, which are recommended before undertaking metagenomic projects with big sample
420 size.

421 **6 Data and Code Availability**

422 Scripts used for the analyses are available at [github](#). Metagenomic datasets involved in this project cannot
423 be made available publicly since they are yet to be formally published.

References

- Ahmed Abdelfattah, Antonino Malacrino, Michael Wisniewski, Santa O Cacciola, and Leonardo Schena. Metabarcoding: A powerful tool to investigate microbial communities and shape future plant protection strategies. *Biological Control*, 120:1–10, 2018.
- Sahar Abubucker, Nicola Segata, Johannes Goll, Alyxandria M Schubert, Jacques Izard, Brandi L Cantarel, Beltran Rodriguez-Mueller, Jeremy Zucker, Mathangi Thiagarajan, Bernard Henrissat, et al. Metabolic reconstruction for metagenomic data and its application to the human microbiome. *PLoS computational biology*, 8(6):e1002358, 2012.
- Antton Alberdi and M Thomas P Gilbert. A guide to the application of hill numbers to dna-based diversity analyses. *Molecular ecology resources*, 19(4):804–817, 2019.
- David R Anderson. *Model based inference in the life sciences: a primer on evidence*. Springer Science & Business Media, 2007.
- Simon Andrews et al. Fastqc: a quality control tool for high throughput sequence data, 2010.
- Kathrin P Aßhauer, Bernd Wemheuer, Rolf Daniel, and Peter Meinicke. Tax4fun: predicting functional profiles from metagenomic 16s rRNA data. *Bioinformatics*, 31(17):2882–2884, 2015.
- Martin Ayling, Matthew D Clark, and Richard M Leggett. New approaches for metagenome assembly with short reads. *Briefings in bioinformatics*, 21(2):584–594, 2020.
- Leslie Bailey. Honey bee pathology. *Annual review of entomology*, 13(1):191–212, 1968.
- Svenja Bänisch, Teja Tscharntke, Doreen Gabriel, and Catrin Westphal. Crop pollination services: complementary resource use by social vs solitary bees facing crops with contrasting flower supply. *Journal of Applied Ecology*, 58(3):476–485, 2021.
- Daniela Becker, Denny Popp, Hauke Harms, and Florian Centler. A modular metagenomics pipeline allowing for the inclusion of prior knowledge using the example of anaerobic digestion. *Microorganisms*, 8(5):669, 2020.
- Anthony M Bolger, Marc Lohse, and Bjoern Usadel. Trimmomatic: a flexible trimmer for illumina sequence data. *Bioinformatics*, 30(15):2114–2120, 2014.
- Germán Bonilla-Rosso, Théodora Steiner, Fabienne Wichmann, Evan Bexkens, and Philipp Engel. Honey bees harbor a diverse gut virome engaging in nested strain-level interactions with the microbiota. *Proceedings of the National Academy of Sciences*, 117(13):7355–7362, 2020.

453 Samuele Bovo, Anisa Ribani, Valerio Joe Utzeri, Giuseppina Schiavo, Francesca Bertolini, and Luca
454 Fontanesi. Shotgun metagenomics of honey dna: Evaluation of a methodological approach to describe
455 a multi-kingdom honey bee derived environmental dna signature. *PLoS One*, 13(10):e0205575, 2018.

456 Samuele Bovo, Valerio Joe Utzeri, Anisa Ribani, Riccardo Cabbri, and Luca Fontanesi. Shotgun se-
457 quencing of honey dna can describe honey bee derived environmental signatures and the honey bee
458 hologenome complexity. *Scientific reports*, 10(1):1–17, 2020.

459 Michael A Brockhurst, Ellie Harrison, James PJ Hall, Thomas Richards, Alan McNally, and Craig
460 MacLean. The ecology and evolution of pangenomes. *Current Biology*, 29(20):R1094–R1103, 2019.

461 Mark JF Brown and Robert J Paxton. The conservation of bees: a global perspective. *Apidologie*, 40(3):
462 410–416, 2009.

463 Benjamin Buchfink, Chao Xie, and Daniel H Huson. Fast and sensitive protein alignment using diamond.
464 *Nature methods*, 12(1):59–60, 2015.

465 Brian Bushnell. Bbmap: a fast, accurate, splice-aware aligner. Technical report, Lawrence Berkeley
466 National Lab.(LBNL), Berkeley, CA (United States), 2014.

467 Brandi L Cantarel, Pedro M Coutinho, Corinne Rancurel, Thomas Bernard, Vincent Lombard, and
468 Bernard Henrissat. The carbohydrate-active enzymes database (cazy): an expert resource for glycoge-
469 nomics. *Nucleic acids research*, 37(suppl_1):D233–D238, 2009.

470 Daniel P Cariveau, J Elijah Powell, Hauke Koch, Rachael Winfree, and Nancy A Moran. Variation in
471 gut microbial communities and its association with pathogen infection in wild bumble bees (*bombus*).
472 *The ISME journal*, 8(12):2369–2379, 2014.

473 Rogan Carr and Elhanan Borenstein. Comparative analysis of functional metagenomic annotation and
474 the mappability of short reads. *PloS one*, 9(8):e105776, 2014.

475 Federica Cattonaro, Alessandro Spadotto, Slobodanka Radovic, and Fabio Marroni. Do you cov me?
476 effect of coverage reduction on metagenome shotgun sequencing studies. *F1000Research*, 7, 2018.

477 Anne Chao and Lou Jost. Coverage-based rarefaction and extrapolation: standardizing samples by
478 completeness rather than size. *Ecology*, 93(12):2533–2547, 2012.

479 Anne Chao, Chun-Huo Chiu, and Lou Jost. Unifying species diversity, phylogenetic diversity, functional
480 diversity, and related similarity and differentiation measures through hill numbers. *Annual review of*
481 *ecology, evolution, and systematics*, 45:297–324, 2014a.

482 Anne Chao, Nicholas J Gotelli, TC Hsieh, Elizabeth L Sander, KH Ma, Robert K Colwell, and Aaron M
483 Ellison. Rarefaction and extrapolation with hill numbers: a framework for sampling and estimation in
484 species diversity studies. *Ecological monographs*, 84(1):45–67, 2014b.

485 Robin L Chazdon, Robert K Colwell, Julie S Denslow, and Manuel R Guariguata. Statistical methods for
486 estimating species richness of woody regeneration in primary and secondary rain forests of northeastern
487 costa rica. 1998.

488 Wenda Cheng and Louise Ashton. Ecology: What affects the distribution of global bee diversity. *Current*
489 *Biology*, 31(3):R127–R128, 2021.

490 Harry K Clench. How to make regional lists of butterflies: some thoughts. *Journal of the Lepidopterists’*
491 *Society*, 1979.

492 Robert K Colwell and Jonathan A Coddington. Estimating terrestrial biodiversity through extrapolation.
493 *Philosophical Transactions of the Royal Society of London. Series B: Biological Sciences*, 345(1311):
494 101–118, 1994.

495 Gene Ontology Consortium. The gene ontology (go) database and informatics resource. *Nucleic acids*
496 *research*, 32(suppl_1):D258–D261, 2004.

497 Samantha M Cook, Caroline S Awmack, Darren A Murray, and Ingrid H Williams. Are honey bees’
498 foraging preferences affected by pollen amino acid composition? *Ecological Entomology*, 28(5):622–627,
499 2003.

500 Otto X Cordero and Martin F Polz. Explaining microbial genomic diversity in light of evolutionary
501 ecology. *Nature Reviews Microbiology*, 12(4):263–273, 2014.

502 Eamonn P Culligan, Roy D Sleator, Julian R Marchesi, and Colin Hill. Metagenomics and novel gene
503 discovery: promise and potential for novel therapeutics. *Virulence*, 5(3):399–412, 2014.

504 Gavin M Douglas, Robert G Beiko, and Morgan GI Langille. Predicting the functional potential of the
505 microbiome from marker genes using picrust. In *Microbiome Analysis*, pages 169–177. Springer, 2018.

506 Stephan Durrer and Paul Schmid-Hempel. Shared use of flowers leads to horizontal pathogen transmission.
507 *Proceedings of the Royal Society of London. Series B: Biological Sciences*, 258(1353):299–302, 1994.

508 Julia Ebeling, Henriette Knispel, Gillian Hertlein, Anne Fünfhaus, and Elke Genersch. Biology of paeni-
509 bacillus larvae, a deadly pathogen of honey bee larvae. *Applied microbiology and biotechnology*, 100
510 (17):7387–7395, 2016.

511 Paul B Eckburg, Elisabeth M Bik, Charles N Bernstein, Elizabeth Purdom, Les Dethlefsen, Michael
512 Sargent, Steven R Gill, Karen E Nelson, and David A Relman. Diversity of the human intestinal
513 microbial flora. *science*, 308(5728):1635–1638, 2005.

514 Kirsten M Ellegaard, Shota Suenami, Ryo Miyazaki, and Philipp Engel. Vast differences in strain-level
515 diversity in the gut microbiota of two closely related honey bee species. *Current Biology*, 30(13):
516 2520–2531, 2020.

517 Akihito Endo and Leon MT Dicks. The genus fructobacillus. *Lactic acid bacteria: biodiversity and*
518 *taxonomy*, pages 381–389, 2014.

519 Philipp Engel, Vincent G Martinson, and Nancy A Moran. Functional diversity within the simple gut
520 microbiota of the honey bee. *Proceedings of the National Academy of Sciences*, 109(27):11002–11007,
521 2012.

522 Philipp Engel, Waldan K Kwong, Quinn McFrederick, Kirk E Anderson, Seth Michael Barribeau,
523 James Angus Chandler, R Scott Cornman, Jacques Dainat, Joachim R De Miranda, Vincent Doublet,
524 et al. The bee microbiome: impact on bee health and model for evolution and ecology of host-microbe
525 interactions. *MBio*, 7(2):e02164–15, 2016.

526 Christiane Essoh, Libera Latino, Cédric Midoux, Yann Blouin, Guillaume Loukou, Simon-Pierre A
527 Nguetta, Serge Lathro, Arsher Cablanmian, Athanase K Kouassi, Gilles Vergnaud, et al. Investigation
528 of a large collection of pseudomonas aeruginosa bacteriophages collected from a single environmental
529 source in abidjan, côte d’ivoire. *PloS one*, 10(6):e0130548, 2015.

530 Laura L Figueroa, Malcolm Blinder, Cali Grincavitch, Angus Jelinek, Emilia K Mann, Liam A Merva,
531 Lucy E Metz, Amy Y Zhao, Rebecca E Irwin, Scott H McArt, et al. Bee pathogen transmission
532 dynamics: deposition, persistence and acquisition on flowers. *Proceedings of the Royal Society B*, 286
533 (1903):20190603, 2019.

534 Eva Forsgren, Tobias C Olofsson, Alejandra Váasquez, and Ingemar Fries. Novel lactic acid bacteria
535 inhibiting paenibacillus larvae in honey bee larvae. *Apidologie*, 41(1):99–108, 2010.

536 Jessica Galloway-Peña and Blake Hanson. Tools for analysis of the microbiome. *Digestive diseases and*
537 *sciences*, 65(3):674–685, 2020.

538 Christina Geldert, Zaid Abdo, Jane E Stewart, and Arathi HS. Dietary supplementation with phytochem-
539 icals improves diversity and abundance of honey bee gut microbiota. *Journal of Applied Microbiology*,
540 130(5):1705–1720, 2021.

541 José Antonio Gómez-Anaya, Rodolfo Novelo-Gutiérrez, Alonso Ramírez, and Roberto Arce-Pérez. Using
542 empirical field data of aquatic insects to infer a cut-off slope value in asymptotic models to assess
543 inventories completeness. *Revista mexicana de biodiversidad*, 85(1):218–227, 2014.

544 Peter Graystock, Dave Goulson, and William OH Hughes. Parasites in bloom: flowers aid dispersal and
545 transmission of pollinator parasites within and between bee species. *Proceedings of the Royal Society*
546 *B: Biological Sciences*, 282(1813):20151371, 2015.

547 Peter Graystock, Wee Hao Ng, Kyle Parks, Amber D Tripodi, Paige A Muñiz, Ashley A Fersch, Christo-
548 pher R Myers, Quinn S McFrederick, and Scott H McArt. Dominant bee species and floral abundance
549 drive parasite temporal dynamics in plant-pollinator communities. *Nature ecology & evolution*, 4(10):
550 1358–1367, 2020.

551 Antonius Petrus de Groot. Protein and amino acid requirements of the honeybee (*apis mellifica* l.). 1953.

552 CBOL Plant Working Group, Peter M Hollingsworth, Laura L Forrest, John L Spouge, Mehrdad Ha-
553 jibabaei, Sujeewan Ratnasingham, Michelle van der Bank, Mark W Chase, Robyn S Cowan, David L
554 Erickson, et al. A dna barcode for land plants. *Proceedings of the National Academy of Sciences*, 106
555 (31):12794–12797, 2009.

556 H Soon Gweon, Liam P Shaw, Jeremy Swann, Nicola De Maio, Manal AbuOun, Rene Niehus, Alasdair TM
557 Hubbard, Mike J Bowes, Mark J Bailey, Tim EA Peto, et al. The impact of sequencing depth on
558 the inferred taxonomic composition and amr gene content of metagenomic samples. *Environmental*
559 *Microbiome*, 14(1):1–15, 2019.

560 Hidenori Hayashi, Mitsuo Sakamoto, and Yoshimi Benno. Phylogenetic analysis of the human gut mi-
561 crobiota using 16s rdna clone libraries and strictly anaerobic culture-based methods. *Microbiology and*
562 *immunology*, 46(8):535–548, 2002.

563 Paul DN Hebert, Sujeewan Ratnasingham, and Jeremy R De Waard. Barcoding animal life: cytochrome c
564 oxidase subunit 1 divergences among closely related species. *Proceedings of the Royal Society of London.*
565 *Series B: Biological Sciences*, 270(suppl.1):S96–S99, 2003.

566 Kenneth L Heck Jr, Gerald van Belle, and Daniel Simberloff. Explicit calculation of the rarefaction
567 diversity measurement and the determination of sufficient sample size. *Ecology*, 56(6):1459–1461, 1975.

568 Harmen P Hendriksma and Sharoni Shafir. Honey bee foragers balance colony nutritional deficiencies.
569 *Behavioral Ecology and Sociobiology*, 70(4):509–517, 2016.

570 Harmen P Hendriksma, Karmi L Oxman, and Sharoni Shafir. Amino acid and carbohydrate tradeoffs
571 by honey bee nectar foragers and their implications for plant–pollinator interactions. *Journal of insect*
572 *physiology*, 69:56–64, 2014.

573 Harmen P Hendriksma, Collin D Pachow, and James C Nieh. Effects of essential amino acid supplemen-
574 tation to promote honey bee gland and muscle development in cages and colonies. *Journal of insect*
575 *physiology*, 117:103906, 2019.

576 Mark O Hill. Diversity and evenness: a unifying notation and its consequences. *Ecology*, 54(2):427–432,
577 1973.

578 Joaquín Hortal and Jorge M Lobo. An ed-based protocol for optimal sampling of biodiversity. *Biodiversity*
579 *& Conservation*, 14(12):2913–2947, 2005.

580 Joaquín Hortal, Paulo AV Borges, and Clara Gaspar. Evaluating the performance of species richness
581 estimators: sensitivity to sample grain size. *Journal of animal ecology*, 75(1):274–287, 2006.

582 Peter Hristov, Boyko Neov, Rositsa Shumkova, and Nadezhda Palova. Significance of apoidea as main
583 pollinators. ecological and economic impact and implications for human nutrition. *Diversity*, 12(7):280,
584 2020a.

585 Peter Hristov, Rositsa Shumkova, Nadezhda Palova, and Boyko Neov. Factors associated with honey bee
586 colony losses: a mini-review. *Veterinary Sciences*, 7(4):166, 2020b.

587 Jaime Huerta-Cepas, Kristoffer Forslund, Luis Pedro Coelho, Damian Szklarczyk, Lars Juhl Jensen,
588 Christian Von Mering, and Peer Bork. Fast genome-wide functional annotation through orthology
589 assignment by eggno-mapper. *Molecular biology and evolution*, 34(8):2115–2122, 2017.

590 Jaime Huerta-Cepas, Damian Szklarczyk, Davide Heller, Ana Hernández-Plaza, Sofia K Forslund, Helen
591 Cook, Daniel R Mende, Ivica Letunic, Thomas Rattei, Lars J Jensen, et al. eggno 5.0: a hierarchical,
592 functionally and phylogenetically annotated orthology resource based on 5090 organisms and 2502
593 viruses. *Nucleic acids research*, 47(D1):D309–D314, 2019.

594 Robert M Hughes, Alan T Herlihy, and David V Peck. Sampling efforts for estimating fish species richness
595 in western usa river sites. *Limnologica*, 87:125859, 2021.

596 Daniel H Huson, Alexander F Auch, Ji Qi, and Stephan C Schuster. Megan analysis of metagenomic
597 data. *Genome research*, 17(3):377–386, 2007.

598 Daniel H Huson, Benjamin Albrecht, Caner Bağcı, Irina Bessarab, Anna Gorska, Dino Jolic, and Ro-
 599 han BH Williams. Megan-lr: new algorithms allow accurate binning and easy interactive exploration
 600 of metagenomic long reads and contigs. *Biology direct*, 13(1):1–17, 2018.

601 Alberto Jimenez-Valverde, Silvia Jimenez Mendoza, Jose Martin Cano, and Miguel L Munguira. Compar-
 602 ing relative model fit of several species-accumulation functions to local papilionoidea and hesperioidea
 603 butterfly inventories of mediterranean habitats. In *Arthropod diversity and conservation*, pages 163–176.
 604 Springer, 2006.

605 Minoru Kanehisa and Susumu Goto. Kegg: kyoto encyclopedia of genes and genomes. *Nucleic acids*
 606 *research*, 28(1):27–30, 2000.

607 Karen M Kapheim, Makenna M Johnson, and Maggi Jolley. Composition and acquisition of the micro-
 608 biome in solitary, ground-nesting alkali bees. *Scientific reports*, 11(1):1–11, 2021.

609 Alexander Keller, Quinn S McFrederick, Prarthana Dharampal, Shawn Steffan, Bryan N Danforth, and
 610 Sara D Leonhardt. (more than) hitchhikers through the network: The shared microbiome of bees and
 611 flowers. *Current Opinion in Insect Science*, 2020.

612 Lucie Kešnerová, Roxane Moritz, and Philipp Engel. *Bartonella apis* sp. nov., a honey bee gut symbiont
 613 of the class alphaproteobacteria. *International journal of systematic and evolutionary microbiology*, 66
 614 (1):414–421, 2016.

615 Shaden AM Khalifa, Esraa H Elshafey, Aya A Shetaia, Aida A Abd El-Wahed, Ahmed F Algethami,
 616 Syed G Musharraf, Mohamed F AlAjmi, Chao Zhao, Saad HD Masry, Mohamed M Abdel-Daim, et al.
 617 Overview of bee pollination and its economic value for crop production. *Insects*, 12(8):688, 2021.

618 Hauke Koch and Paul Schmid-Hempel. Bacterial communities in central european bumblebees: low
 619 diversity and high specificity. *Microbial Ecology*, 62(1):121–133, 2011a.

620 Hauke Koch and Paul Schmid-Hempel. Socially transmitted gut microbiota protect bumble bees against
 621 an intestinal parasite. *Proceedings of the National Academy of Sciences*, 108(48):19288–19292, 2011b.

622 Hauke Koch, Mark JF Brown, and Philip C Stevenson. The role of disease in bee foraging ecology. *Current*
 623 *opinion in insect science*, 21:60–67, 2017.

624 Waldan K Kwong, Luis A Medina, Hauke Koch, Kong-Wah Sing, Eunice Jia Yu Soh, John S Ascher,
 625 Rodolfo Jaffé, and Nancy A Moran. Dynamic microbiome evolution in social bees. *Science Advances*,
 626 3(3):e1600513, 2017.

627 Ben Langmead and Steven L Salzberg. Fast gapped-read alignment with bowtie 2. *Nature methods*, 9(4):
628 357, 2012.

629 Fredrick J Lee, Douglas B Rusch, Frank J Stewart, Heather R Mattila, and Irene LG Newton. Saccharide
630 breakdown and fermentation by the honey bee gut microbiome. *Environmental microbiology*, 17(3):
631 796–815, 2015.

632 Fredrick J Lee, Kayla I Miller, James B McKinlay, and Irene LG Newton. Differential carbohydrate
633 utilization and organic acid production by honey bee symbionts. *FEMS microbiology ecology*, 94(8):
634 fiy113, 2018.

635 Dinghua Li, Chi-Man Liu, Ruibang Luo, Kunihiko Sadakane, and Tak-Wah Lam. Megahit: an ultra-
636 fast single-node solution for large and complex metagenomics assembly via succinct de bruijn graph.
637 *Bioinformatics*, 31(10):1674–1676, 2015.

638 Heng Li and Richard Durbin. Fast and accurate short read alignment with burrows–wheeler transform.
639 *bioinformatics*, 25(14):1754–1760, 2009.

640 Heng Li, Bob Handsaker, Alec Wysoker, Tim Fennell, Jue Ruan, Nils Homer, Gabor Marth, Goncalo
641 Abecasis, and Richard Durbin. The sequence alignment/map format and samtools. *Bioinformatics*, 25
642 (16):2078–2079, 2009.

643 Zhanshan Ma and Lianwei Li. Measuring metagenome diversity and similarity with hill numbers. *Molec-
644 ular ecology resources*, 18(6):1339–1355, 2018.

645 Patrick W Maes, Pedro AP Rodrigues, Randy Oliver, Brendon M Mott, and Kirk E Anderson. Diet-
646 related gut bacterial dysbiosis correlates with impaired development, increased mortality and nosema
647 disease in the honeybee (*apis mellifera*). *Molecular Ecology*, 25(21):5439–5450, 2016.

648 Vincent G Martinson, Tanja Magoc, Hauke Koch, Steven L Salzberg, and Nancy A Moran. Genomic
649 features of a bumble bee symbiont reflect its host environment. *Applied and environmental microbiology*,
650 80(13):3793–3803, 2014.

651 Tomonori Matsuzawa, Ryo Kohsaka, and Yuta Uchiyama. Application of environmental dna: Honey
652 bee behavior and ecosystems for sustainable beekeeping. In *Modern beekeeping-bases for sustainable
653 production*. IntechOpen, 2020.

654 QUINN S McFREDERICK, William T Wcislo, Douglas R Taylor, Heather D Ishak, Scot E Dowd, and
655 Ulrich G Mueller. Environment or kin: whence do bees obtain acidophilic bacteria? *Molecular Ecology*,
656 21(7):1754–1768, 2012.

657 Quinn S McFrederick, Jason M Thomas, John L Neff, Hoang Q Vuong, Kaleigh A Russell, Amanda R
 658 Hale, and Ulrich G Mueller. Flowers and wild megachilid bees share microbes. *Microbial ecology*, 73
 659 (1):188–200, 2017.

660 Folker Meyer, Daniel Paarmann, Mark D’Souza, Robert Olson, Elizabeth M Glass, Michael Kubal, Tobias
 661 Paczian, Alex Rodriguez, Rick Stevens, Andreas Wilke, et al. The metagenomics rast server—a public
 662 resource for the automatic phylogenetic and functional analysis of metagenomes. *BMC bioinformatics*,
 663 9(1):1–8, 2008.

664 Paul W Mielke Jr and Earl S Johnson. Some generalized beta distributions of the second kind having
 665 desirable application features in hydrology and meteorology. *Water Resources Research*, 10(2):223–226,
 666 1974.

667 Alla Mikheenko, Vladislav Saveliev, and Alexey Gurevich. Metaquast: evaluation of metagenome assem-
 668 blies. *Bioinformatics*, 32(7):1088–1090, 2016.

669 Ronald I Miller and Richard G Wiegert. Documenting completeness, species-area relations, and the species-
 670 abundance distribution of a regional flora. *Ecology*, 70(1):16–22, 1989.

671 Nancy A Moran. Genomics of the honey bee microbiome. *Current opinion in insect science*, 10:22–28,
 672 2015.

673 Felicia N New and Ilana L Brito. What is metagenomics teaching us, and what is missed? *Annual Review*
 674 *of Microbiology*, 74:117–135, 2020.

675 Sergey I Nikolenko, Anton I Korobeynikov, and Max A Alekseyev. Bayeshammer: Bayesian clustering for
 676 error correction in single-cell sequencing. In *BMC genomics*, volume 14, pages 1–11. Springer, 2013.

677 R Henrik Nilsson, Erik Kristiansson, Martin Ryberg, Nils Hallenberg, and Karl-Henrik Larsson. Intraspe-
 678 cific its variability in the kingdom fungi as expressed in the international sequence databases and its
 679 implications for molecular species identification. *Evolutionary bioinformatics*, 4:EBO–S653, 2008.

680 Sergey Nurk, Dmitry Meleshko, Anton Korobeynikov, and Pavel A Pevzner. metaspades: a new versatile
 681 metagenomic assembler. *Genome research*, 27(5):824–834, 2017.

682 Pier P Paoli, Luisa A Wakeling, Geraldine A Wright, and Dianne Ford. The dietary proportion of essential
 683 amino acids and sir2 influence lifespan in the honeybee. *Age*, 36(3):1239–1247, 2014.

684 K Papadopoulou-Karabela, N Iliadis, V Liakos, and E Bourdzy-Hatzopoulou. Experimental infection of
 685 honeybees by pseudomonas aeruginosa. *Apidologie*, 23(5):393–397, 1992.

686 K Papadopoulou-Karabela, N Iliadis, and V Liakos. Haemocyte changes in honeybee (*Apis mellifera* L.)
687 artificially infected by *Pseudomonas aeruginosa*. *Apidologie*, 24(1):81–86, 1993.

688 Yu Peng, Henry CM Leung, Siu-Ming Yiu, and Francis YL Chin. IdBA-UD: a de novo assembler for single-
689 cell and metagenomic sequencing data with highly uneven depth. *Bioinformatics*, 28(11):1420–1428,
690 2012.

691 Judit J Péntzes, Maria Söderlund-Venermo, Marta Canuti, Anna Maria Eis-Hübinger, Joseph Hughes,
692 Susan F Cotmore, and Balázs Harrach. Reorganizing the family Parvoviridae: a revised taxonomy
693 independent of the canonical approach based on host association. *Archives of Virology*, 165(9):2133–
694 2146, 2020.

695 Joana Pereira-Marques, Anne Hout, Rui M Ferreira, Michiel Weber, Ines Pinto-Ribeiro, Leen-Jan van
696 Doorn, Cornelis Willem Knetsch, and Ceu Figueiredo. Impact of host DNA and sequencing depth
697 on the taxonomic resolution of whole metagenome sequencing for microbiome analysis. *Frontiers in*
698 *Microbiology*, 10:1277, 2019.

699 Elijah Powell, Nalin Ratnayeke, and Nancy A Moran. Strain diversity and host specificity in a specialized
700 gut symbiont of honeybees and bumblebees. *Molecular ecology*, 25(18):4461–4471, 2016.

701 J Elijah Powell, Zac Carver, Sean P Leonard, and Nancy A Moran. Field-realistic tylosin exposure
702 impacts honey bee microbiota and pathogen susceptibility, which is ameliorated by native gut probiotics.
703 *Microbiology Spectrum*, 9(1):e00103–21.

704 Andrey Prjibelski, Dmitry Antipov, Dmitry Meleshko, Alla Lapidus, and Anton Korobeynikov. Using
705 SPAdes de novo assembler. *Current Protocols in Bioinformatics*, 70(1):e102, 2020.

706 Christopher Quince, Alan W Walker, Jared T Simpson, Nicholas J Loman, and Nicola Segata. Shotgun
707 metagenomics, from sampling to analysis. *Nature biotechnology*, 35(9):833–844, 2017.

708 Aaron R Quinlan and Ira M Hall. BEDTools: a flexible suite of utilities for comparing genomic features.
709 *Bioinformatics*, 26(6):841–842, 2010.

710 David Ratkowsky. Nonlinear regression modelling. 1983.

711 David A Ratkowsky and David EA Giles. *Handbook of nonlinear regression models*. Number 04; QA278.
712 2, R3. M. Dekker New York, 1990.

713 Kasie Raymann and Nancy A Moran. The role of the gut microbiome in health and disease of adult honey
714 bee workers. *Current opinion in insect science*, 26:97–104, 2018.

715 Anisa Ribani, Valerio Joe Utzeri, Valeria Taurisano, and Luca Fontanesi. Honey as a source of environ-
716 mental dna for the detection and monitoring of honey bee pathogens and parasites. *Veterinary sciences*,
717 7(3):113, 2020.

718 Michael Roswell, Jonathan Dushoff, and Rachael Winfree. A conceptual guide to measuring species
719 diversity. *Oikos*, 130(3):321–338, 2021.

720 Jason A Rothman, Laura Leger, Peter Graystock, Kaleigh Russell, and Quinn S McFrederick. The bumble
721 bee microbiome increases survival of bees exposed to selenate toxicity. *Environmental microbiology*, 21
722 (9):3417–3429, 2019a.

723 Jason A Rothman, Laura Leger, Jay S Kirkwood, and Quinn S McFrederick. Cadmium and selenate
724 exposure affects the honey bee microbiome and metabolome, and bee-associated bacteria show potential
725 for bioaccumulation. *Applied and environmental microbiology*, 85(21):e01411–19, 2019b.

726 Jason A Rothman, Kaleigh A Russell, Laura Leger, Quinn S McFrederick, and Peter Graystock. The
727 direct and indirect effects of environmental toxicants on the health of bumblebees and their microbiomes.
728 *Proceedings of the Royal Society B*, 287(1937):20200980, 2020.

729 Alexander Sczyrba, Peter Hofmann, Peter Belmann, David Koslicki, Stefan Janssen, Johannes Dröge,
730 Ivan Gregor, Stephan Majda, Jessika Fiedler, Eik Dahms, et al. Critical assessment of metagenome
731 interpretation benchmark of metagenomics software. *Nature methods*, 14(11):1063–1071, 2017.

732 Itai Sharon, Michael Kertesz, Laura A Hug, Dmitry Pushkarev, Timothy A Blauwkamp, Cindy J Castelle,
733 Mojgan Amirebrahimi, Brian C Thomas, David Burstein, Susannah G Tringe, et al. Accurate, multi-kb
734 reads resolve complex populations and detect rare microorganisms. *Genome research*, 25(4):534–543,
735 2015.

736 Nicola K Simcock, Helen E Gray, and Geraldine A Wright. Single amino acids in sucrose rewards modulate
737 feeding and associative learning in the honeybee. *Journal of insect physiology*, 69:41–48, 2014.

738 Daniel Stabler, Pier P Paoli, Susan W Nicolson, and Geraldine A Wright. Nutrient balancing of the adult
739 worker bumblebee (*bombus terrestris*) depends on the dietary source of essential amino acids. *The*
740 *Journal of experimental biology*, 218(5):793–802, 2015.

741 Javier Tamames and Fernando Puente-Sánchez. Squeezemeta, a highly portable, fully automatic metage-
742 nomic analysis pipeline. *Frontiers in microbiology*, 9:3349, 2019.

743 Roman L Tatusov, Michael Y Galperin, Darren A Natale, and Eugene V Koonin. The cog database: a
744 tool for genome-scale analysis of protein functions and evolution. *Nucleic acids research*, 28(1):33–36,
745 2000.

746 Michelle A Taylor, Alastair W Robertson, Patrick J Biggs, Kate K Richards, Daniel F Jones, and Shan-
747 thi G Parkar. The effect of carbohydrate sources: Sucrose, invert sugar and components of mānuka
748 honey, on core bacteria in the digestive tract of adult honey bees (*apis mellifera*). *PloS one*, 14(12):
749 e0225845, 2019.

750 Quang Tran and Vinhthuy Phan. Assembling reads improves taxonomic classification of species. *Genes*,
751 11(8):946, 2020.

752 Susannah Green Tringe, Christian Von Mering, Arthur Kobayashi, Asaf A Salamov, Kevin Chen, Hwai W
753 Chang, Mircea Podar, Jay M Short, Eric J Mathur, John C Detter, et al. Comparative metagenomics
754 of microbial communities. *Science*, 308(5721):554–557, 2005.

755 Rachel L Vannette. The floral microbiome: plant, pollinator, and microbial perspectives. *Annual Review*
756 *of Ecology, Evolution, and Systematics*, 51:363–386, 2020.

757 Louise Vermote, Marko Verce, Luc De Vuyst, and Stefan Weckx. Amplicon and shotgun metagenomic
758 sequencing indicates that microbial ecosystems present in cheese brines reflect environmental inoculation
759 during the cheese production process. *International Dairy Journal*, 87:44–53, 2018.

760 John Vollmers, Sandra Wiegand, and Anne-Kristin Kaster. Comparing and evaluating metagenome
761 assembly tools from a microbiologists perspective-not only size matters! *PloS one*, 12(1):e0169662,
762 2017.

763 Kai Wang, Jiahuan Li, Liuwei Zhao, Xiyan Mu, Chen Wang, Miao Wang, Xiaofeng Xue, Suzhen Qi, and
764 Liming Wu. Gut microbiota protects honey bees (*apis mellifera* l.) against polystyrene microplastics
765 exposure risks. *Journal of Hazardous Materials*, 402:123828, 2021.

766 Edwin C Webb et al. *Enzyme nomenclature 1992. Recommendations of the Nomenclature Committee of*
767 *the International Union of Biochemistry and Molecular Biology on the Nomenclature and Classification*
768 *of Enzymes*. Number Ed. 6. Academic Press, 1992.

769 K Eric Wommack, Jaysheel Bhavsar, and Jacques Ravel. Metagenomics: read length matters. *Applied*
770 *and environmental microbiology*, 74(5):1453–1463, 2008.

771 Derrick E Wood and Steven L Salzberg. Kraken: ultrafast metagenomic sequence classification using
772 exact alignments. *Genome biology*, 15(3):1–12, 2014.

773 Yuzhen Ye and Thomas G Doak. A parsimony approach to biological pathway reconstruction/inference
774 for genomes and metagenomes. *PLoS computational biology*, 5(8):e1000465, 2009.

775 Nicholas D Youngblut, Jacobo De la Cuesta-Zuluaga, Georg H Reischer, Silke Dauser, Nathalie Schuster,
776 Chris Walzer, Gabrielle Stalder, Andreas H Farnleitner, and Ruth E Ley. Large-scale metagenome as-
777 sembly reveals novel animal-associated microbial genomes, biosynthetic gene clusters, and other genetic
778 diversity. *Msystems*, 5(6):e01045–20, 2020.

779 Rahat Zaheer, Noelle Noyes, Rodrigo Ortega Polo, Shaun R Cook, Eric Marinier, Gary Van Domselaar,
780 Keith E Belk, Paul S Morley, and Tim A McAllister. Impact of sequencing depth on the characterization
781 of the microbiome and resistome. *Scientific reports*, 8(1):1–11, 2018.

782 Eduardo E Zattara and Marcelo A Aizen. Worldwide occurrence records suggest a global decline in bee
783 species richness. *One Earth*, 4(1):114–123, 2021.

784 Hao Zheng, Julie Perreau, J Elijah Powell, Benfeng Han, Zijiang Zhang, Waldan K Kwong, Susannah G
785 Tringe, and Nancy A Moran. Division of labor in honey bee gut microbiota for plant polysaccharide
786 digestion. *Proceedings of the National Academy of Sciences*, 116(51):25909–25916, 2019.

787 Jinshui Zheng, Stijn Wittouck, Elisa Salvetti, Charles MAP Franz, Hugh Harris, Paola Mattarelli, Paul W
788 O’Toole, Bruno Pot, Peter Vandamme, Jens Walter, et al. A taxonomic note on the genus *Lactobacillus*:
789 Description of 23 novel genera, emended description of the genus *Lactobacillus* Beijerinck 1901, and union
790 of *Lactobacillaceae* and *Leuconostocaceae*. 2020.

7 Supplementary

7.1 Parameter settings of integrated pipeline

7.1.1 Quality control and host removing

Raw data quality control was conducted to reduce compromise from low-quality reads. Raw data quality was checked using FastQC v.0.11.5 (Andrews et al., 2010) before filtering. FastQC reports of raw reads showed the following aspects need to be covered in quality control: (1) low base quality in 3'-end (Figure S1a); (2) uneven base content in 5'-end (Figure S1c) and (3) the present of Nextera adaptors (Figure S1e). Therefore, raw reads were filtered using Trimmomatic v.0.39 (Bolger et al., 2014), which (1) trimmed adaptors; (2) cutted 15 bases from the 5'-ends of reads; (3) cut bases off from 3'-ends of reads if Phred-33 quality is below 20; (4) dropped reads shorter than 50 bp; (5) dropped reads if average Phred-33 quality is below 20. Then unpaired reads were removed and quality of clean data was checked using FastQC (Figure S1d, S1e, S1f).

After quality control, host read pairs were removed. First, clean read pairs were mapped to host genome (GCA_003254395.2 for *Apis mellifera* and GCA_000188095 for *Bombus impatiens*, downloaded from NCBI) using Bowtie2 v.2.4.2 (Langmead and Salzberg, 2012) with flags *-end-to-end* and *-sensitive*. With flag *-end-to-end*, Bowtie2 requires the read aligned without any clipping from neither end, and *-sensitive* maintains a trade-off between speed and sensitivity. SAM files generated by Bowtie2 were converted to BAM format using SAMtools v.1.11 (Li et al., 2009). Then non-host read pairs were extracted from BAM files by SAMtools according to the present of SAM flag 12 (neither forward nor reverse read in a pair of reads is mapped).

7.1.2 Assembly-dependent species identification

In order to identify taxa of metagenome, *de novo* assembly was conducted. Non-host read pairs were assembled using SPAdes v.3.15.2 (Prjibelski et al., 2020). Values of k-mer ranged from 21 to 101 at interval of 10. Flags *-only-assembler* and *-meta* were used. Through flag *-meta*, SPAdes runs metaSPAdes which is developed for metagenomic assembly (Nurk et al., 2017). The *-only-assembler* flag skips read error correction and runs assembly only. Its utilization is justified by the following facts. First, when *-only-assembler* is not used, SPAdes conducts error correction before assembly. It is conducted by BayesHamme, which is optimized for single cell sequencing instead of shotgun metagenomics (Nikolenko et al., 2013). Besides, reads used for *de novo* assembly had been filtered to ensure their quality.

After assembly, taxon identification was conducted using DIAMOND v.2.0.7.145 (Buchfink et al., 2015) and MEGAN6 (Huson et al., 2007). Assembled contigs with a length above 500 bp were aligned to

nr database using DIAMOND v.2.0.7.145 with *-long-reads* flag. This flag triggers frame-shift aware alignment mode, which is optimized for long sequence alignment. Therefore, short contigs (length < 500 bp) were not retained. Besides, alignments with an E-value < $1e - 5$ or identity < 50% were removed, and for each contig, only alignments above 10% of the best local bit score were retained. The output of DIAMOND was analysed by the *blast2rma* tool of MEGAN6 with *-lg* flag, which runs lowest-common-ancestor (LCA)-based algorithm developed for long contigs and assigns each contig to a taxon (Huson et al., 2018). The parameter *-supp* was 0, which means the present of a taxon would be identified as long as at least one contig was assigned. This value was used because a contig is assembled from multiple short reads and represents a strong signal for the present of a taxon.

7.1.3 Fragment recruitment

To integrate individual genomic data of species identified by assembly-dependent search, a reference database comprising reference genome dataset, *i.e.* genomic sequences in FASTA format and corresponding gff file, was constructed. For each species represented by assembly, its reference genome dataset, if available, was downloaded from NCBI using its *datasets* command-line tool and added to the reference database.

Then fragment recruitment was conducted. The non-host read pairs were mapped to genomic sequences in the reference database using Bowtie2. Read pairs that were not recruited were extracted using SAMtools. Settings for Bowtie2 and SAMtools were the same as that described in 7.1.1. Read pairs recruited by the reference database were assigned to corresponding species, while the others were subjected to assembly-independent search.

7.1.4 Assembly-independent species identification

In order to detect species not represented by assembly (Sharon et al., 2015, Vollmers et al., 2017), assembly-independent search was conducted, taking read pairs not recruited by the reference database as input. These reads were aligned to nr database through DIAMOND without using *-long-reads* flag, which triggers computing alignments for short metagenomic reads. Other settings were the same as described in 7.1.2. Then the output of DIAMOND was analysed by MEGAN6 (*blast2rma* tool), which assigns read pairs to taxa through LCA algorithm. Here the parameter *-supp* was 0.1, which means a taxon is reported after being represented by at least 0.1% of all assigned read pairs. It was used in order to avoid false positive results.

7.1.5 Functional annotation

Functional annotation was conducted by EggNOG-mapper v.2.1.2 (Huerta-Cepas et al., 2017). Sequences were searched against eggNOG database (Huerta-Cepas et al., 2019) for best seed orthologs using DIAMOND and fine-grained orthology assignments were retrieved from pre-computed eggNOG phylogenetic trees. Then functional descriptions of retrieved orthologs including Gene Ontology (GO) terms (Consortium, 2004), KOs, Enzyme Commission (EC) numbers (Webb et al., 1992), Carbohydrate-Active Enzymes (CAZy) terms (Cantarel et al., 2009) and Clusters of Orthologous Groups (COG) functional categories (Tatusov et al., 2000) were transferred to query sequences.

7.2 Candidate models for fitting rarefaction curves

Table S1: Candidate species accumulation models. Dependent variable $D^{(q)}$ is Hill number of order q and independent variable x is sequencing depth. a, b, c, d are fitted coefficients.

Model	Parameter(k)	Derivative	Asymptote	Reference
$D^{(q)} = \frac{ax}{bx+1}$	2	$\frac{dD^q}{dx} = \frac{a}{(bx+1)^2}$	$\frac{a}{b}$	Clench (1979)
$D^{(q)} = a(1 - e^{-bx})$	2	$\frac{dD^q}{dx} = abe^{-bx}$	a	Miller and Wiegert (1989)
$D^{(q)} = a - bc^x$	3	$\frac{dD^q}{dx} = -bc^x \log(c)$	a	Ratkowsky (1983)
$D^{(q)} = a(1 - e^{-bx})^c$	3	$\frac{dD^q}{dx} = abce^{-bx}(1 - e^{-bx})^{c-1}$	a	Ratkowsky and Giles (1990)
$D^{(q)} = a(1 - (1 + (\frac{x}{c})^d)^{-b})$	4	$\frac{dD^q}{dx} = \frac{abd}{c}(\frac{x}{c})^{d-1}(1 + (\frac{x}{c})^d)^{-b-1}$	a	Mielke Jr and Johnson (1974)

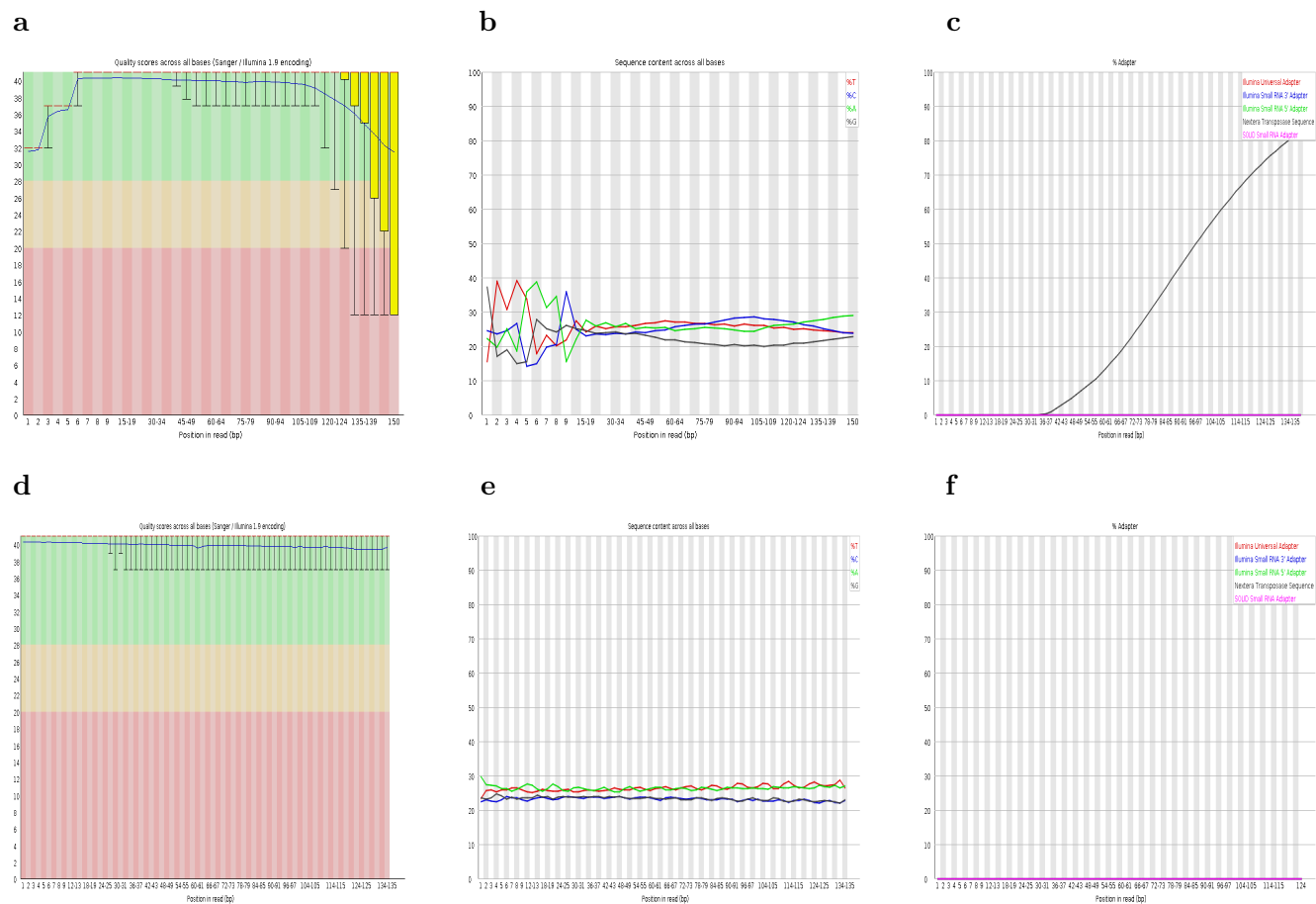


Figure S1: Data quality report of forward reads from bumble bee sample *Bee_Bimpatiens_hv4_1*. a, b and c shows low base quality in 3'-end, uneven base content in 5'-end and present of Nextera adaptors in raw data, respectively. d, e and f shows the same results from clean data.

Table S2: Statistics of sequenced read pairs.

Sample	Host	Raw read pair	Clean read pair	Non-host read pair
			[percentage of raw read pair]	[percentage of clean read pair]
<i>Bee_Amellifera_hv15_1</i>	<i>Apis mellifera</i>	63159968	45059211 [71.34%]	38837759 [86.19%]
<i>Bee_Amellifera_wild_1</i>	<i>Apis mellifera</i>	58113227	44466776 [76.52%]	17014144 [38.26%]
<i>Bee_Amellifera_hv13_2</i>	<i>Apis mellifera</i>	56836899	35282101 [62.08%]	10413704 [29.52%]
<i>Bee_Amellifera_hv13_1</i>	<i>Apis mellifera</i>	1104861	842095 [76.22%]	665507 [79.03%]
<i>Bee_Bimpatiens_hv3_1</i>	<i>Bombus impatiens</i>	63973750	53612702 [83.80%]	5300592 [9.89%]
<i>Bee_Bimpatiens_hv4_1</i>	<i>Bombus impatiens</i>	58988182	48426748 [82.10%]	3557052 [7.35%]
<i>Bee_Bimpatiens_hv4_2</i>	<i>Bombus impatiens</i>	54955553	45805759 [83.35%]	4618023 [10.08%]
<i>Flower_eDNA</i>	None	1443107	882436 [61.15%]	882436 [100%]

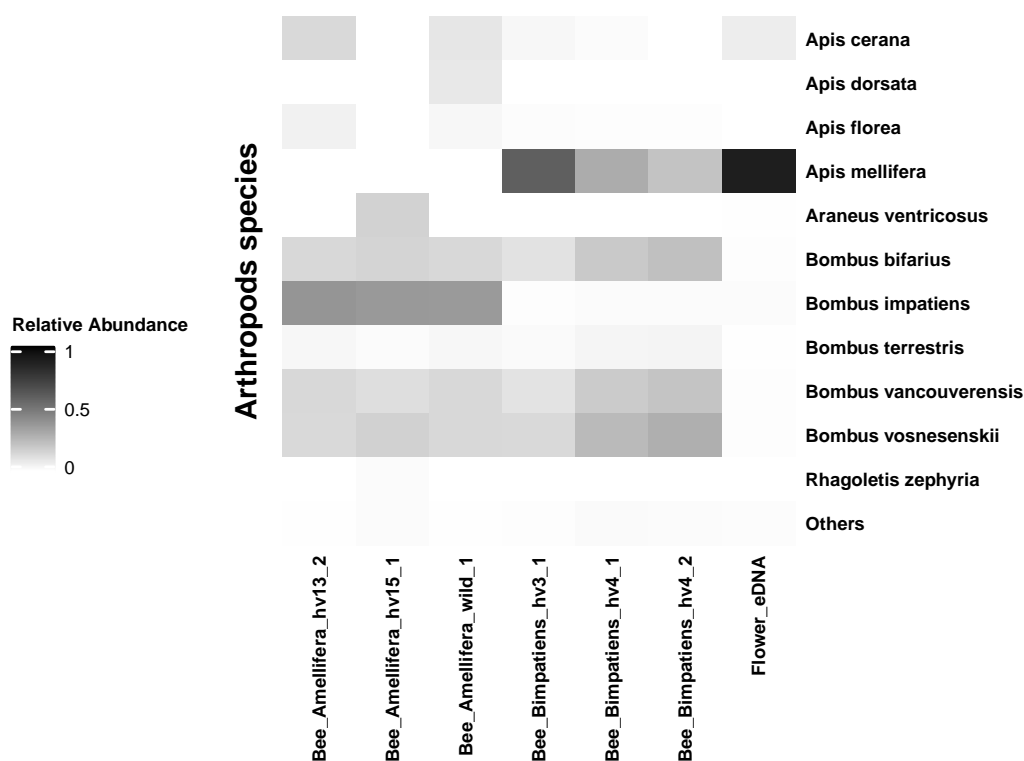


Figure S2: Heatmaps for arthropod species abundance distribution in all samples. The relative abundance takes reads assigned to arthropod species as background. Species with relative abundance smaller than 1% in all samples are collapsed as "others". It should be noted that for bee samples, host contamination was removed before taxon profiling. As a result, the relative abundances of honey bees are extremely low in three honey bee samples, and the same for bumble bees in three bumble bee samples.

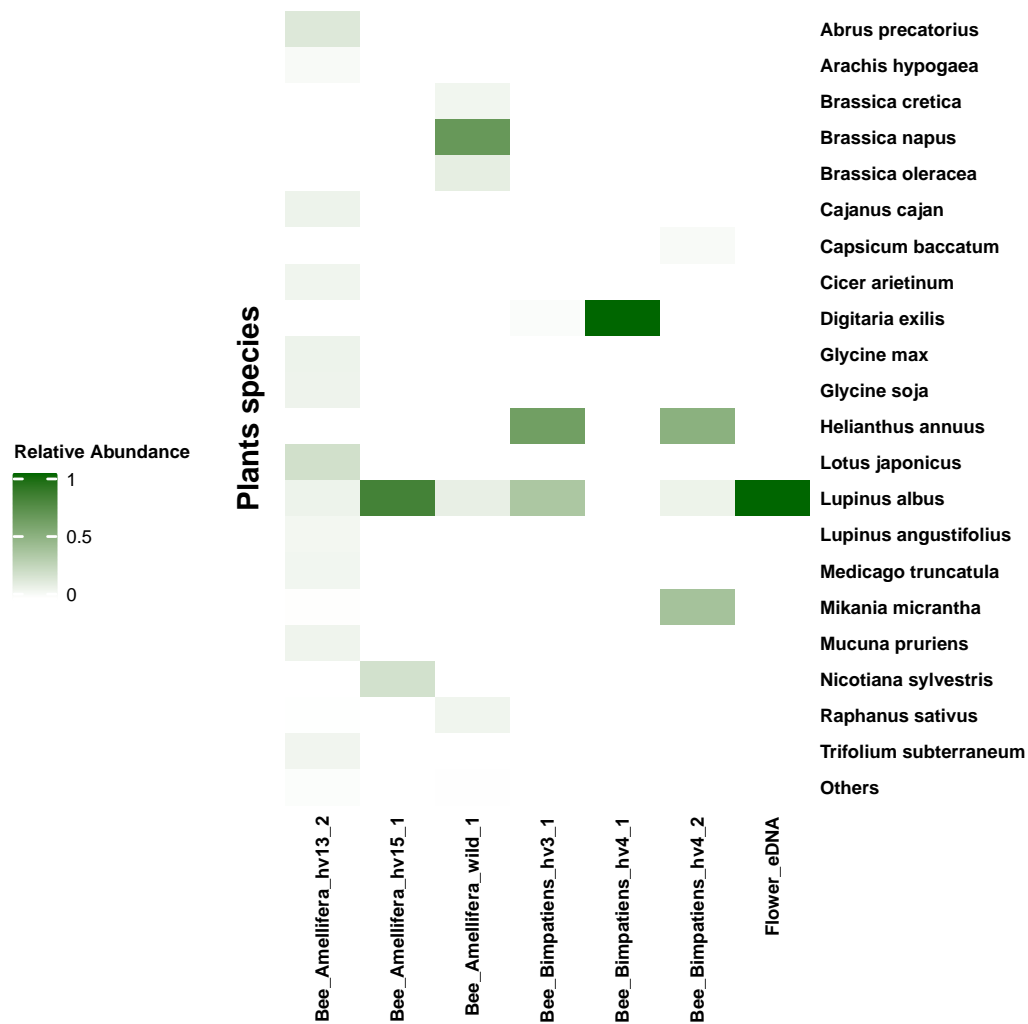


Figure S3: Heatmaps for plant species abundance distribution in all samples. The relative abundance takes reads assigned to plant species as background. Species with relative abundance smaller than 1% in all samples are collapsed as "others".

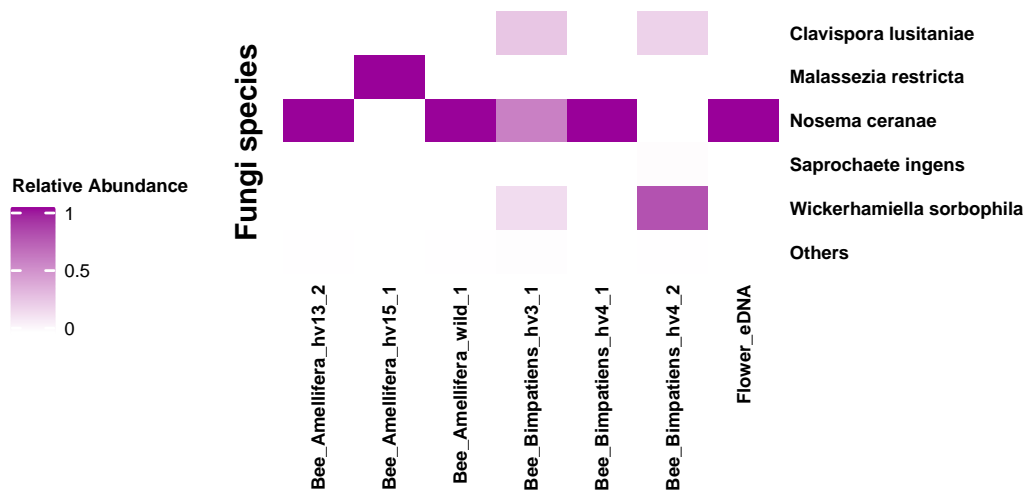


Figure S4: Heatmaps for fungal species abundance distribution in all samples. The relative abundance takes reads assigned to fungal species as background. Species with relative abundance smaller than 1% in all samples are collapsed as "others".

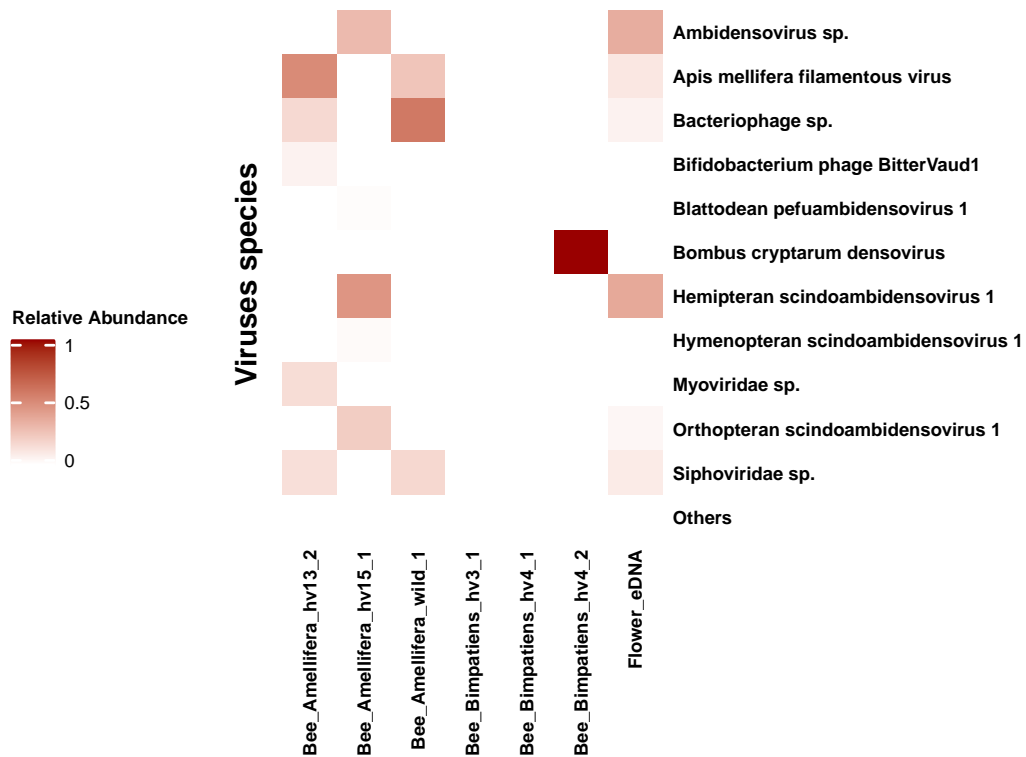


Figure S5: Heatmaps for virus species abundance distribution in all samples. The relative abundance takes reads assigned to virus species as background. Species with relative abundance smaller than 1% in all samples are collapsed as "others".

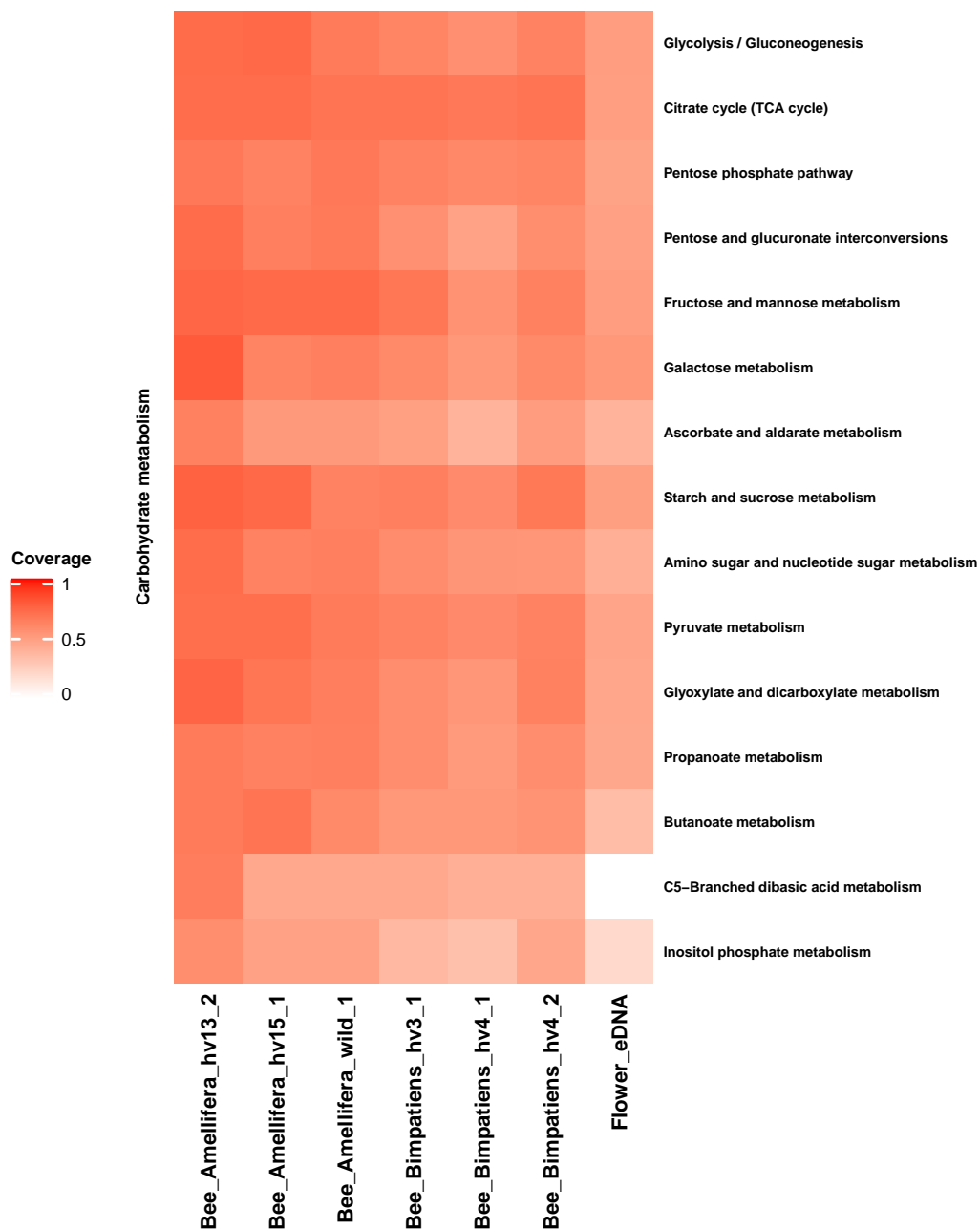


Figure S6: Heatmaps for pathways of carbohydrate metabolism.

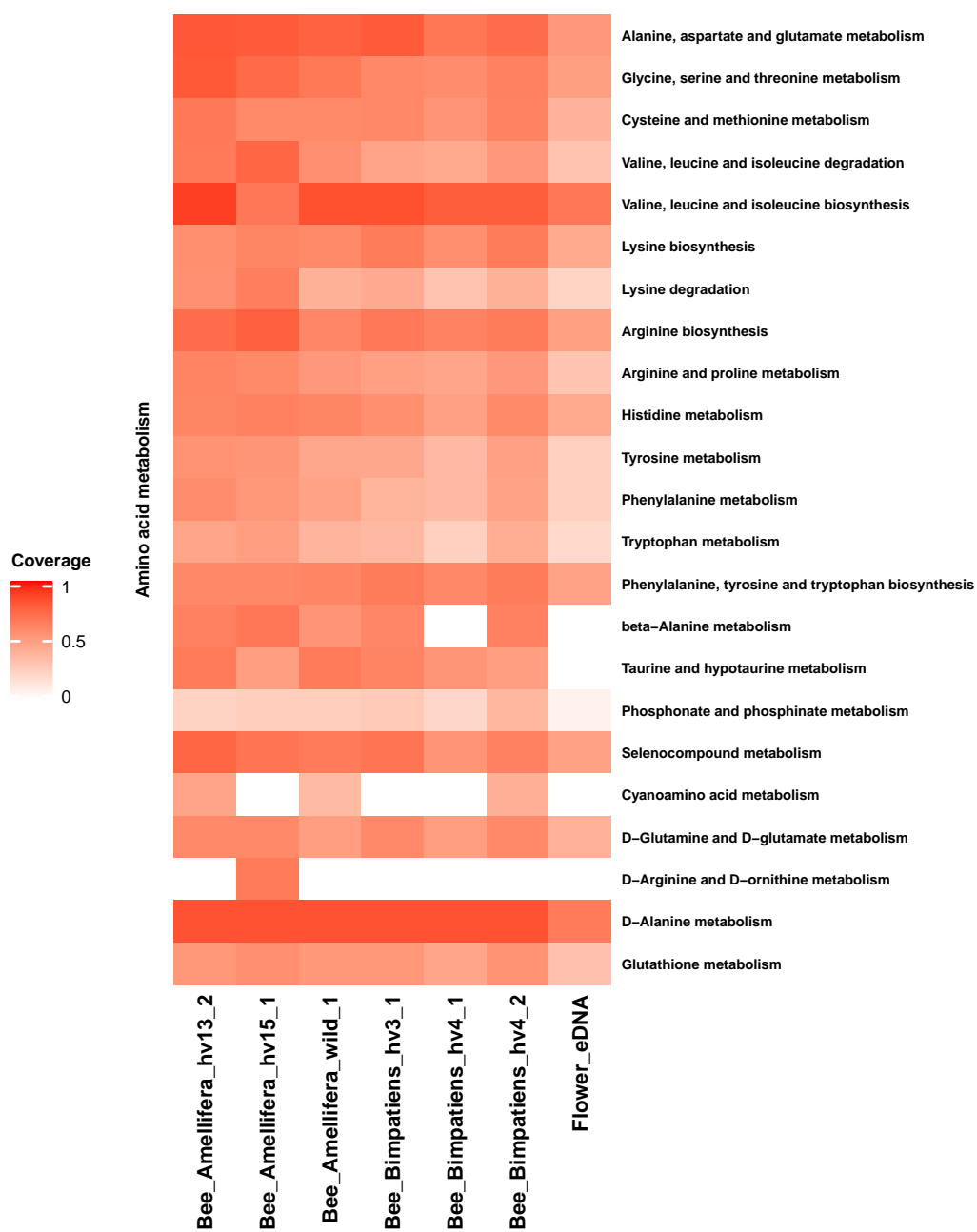


Figure S7: Heatmaps for pathways of amino acid metabolism.